Renewable and Sustainable Energy Reviews 167 (2022) 112796

Contents lists available at ScienceDirect

Renewable and Sustainable Energy Reviews

journal homepage: www.elsevier.com/locate/rser

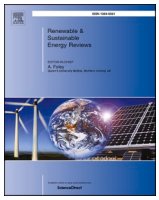

A Review of the Effects of Haze on Solar Photovoltaic Performance

Seyyed Ali Sadat [a], Bram Hoex [b], Joshua M. Pearce [a,c,*]

[a] Department of Electrical & Computer Engineering, Western University, ON, Canada
[b] School of Photovoltaics & Renewable Energy Engineering, UNSW, Australia
[c] Ivey Business School, Western University, London, ON, Canada

ARTICLE INFO

Keywords:
Photovoltaics
Performance assessments
Solar energy generation
Haze concentration
Air pollution
Irradiance

ABSTRACT

Solar photovoltaic (PV) deployments are growing rapidly to provide a sustainable source of electricity, but their output is strongly impacted by environmental phenomena such as soiling and low irradiance conditions induced by haze from urban sources, dust, and bushfire smoke. This review examines the effects of haze on PV performance, highlights significant results, and identifies apparent research gaps in the current literature. In addition to the severe health issues caused by industrial exhausted aerosol, dust storms particles, and bushfire smoke, reduction in irradiance (in some cases up to 80%) is the most dominant impact of these sources of haze. Haze also causes changes in the received solar spectrum, and higher bandgap PV materials are more affected by the presence of haze and aerosols in the atmosphere by 20-40% than low bandgap semiconductors. In many cities throughout the world, pollution-related haze causes substantial annual revenue loss to PV operators. In addition, haze imposes severe effects on direct irradiance; therefore, tracking systems and concentrated PV systems are most affected. These technical impacts of haze all indicate the need for careful customization of PV systems for specific locations. In addition, to increase global PV output, it is clear that air pollution control regulations such as China's national policies against air pollution and eco-friendly international actions such as COP26 should be employed and executed. Further studies are needed including indoor experiments, forecasting future implications of aerosols on PV energy conversion, and performing energy policy analysis to identify associated challenges and propose practical strategies.

1. Introduction

There has been a significant increase in the solar photovoltaic (PV) installed capacity worldwide, increasing from 41 GW in 2010 to 716 GW by the end of 2020 [1], with a continuous trend of exceeding expectations [2, 3]. For example, China has increased capacity from 1 GW in 2010 to 254 GW by 2020, while the United States has progressed from 3 GW PV in 2010 to 74 GW by 2020 [4]. This growth is being driven by the levelized cost of electricity (LCOE) [5], which is highly dependent on long term performance (e.g. lifetimes of 25 years or more [6]). There are numerous threats to the rated performance of PV plants, and how these concerns are addressed is important [7-9] for long-term financing [10, 11]. Among these, environmental factors are one of the most critical challenges. The meteorological conditions strongly impact the output of a PV system at the PV plant's site, which might experience cloudy, rainy, and foggy conditions and reduced solar flux from haze [12]. Whereas these first three meteorological factors are natural, the latter detrimental factor of haze is often caused by humans through particulate matter (PM) pollution that has become a common phenomenon worldwide, especially in metropolitan areas. This PM pollution is due to three causes 1) the high rate of industrial activities and other anthropogenic causes (e.g. urban haze) [13], 2) dust storms in deforested and arid regions [14], and 3) bushfire smoke [15]. The latter of which is now common in some countries during summer, such as the 2019–20 Australian [15] and 2021 British Columbia bushfires seasons [16].

Haze from particles of all three sources can be suspended in air or deposited on surfaces. Urban haze (human-made or anthropogenic) typically consists of sulfur dioxide (SO_2) or sulfate (SO_4) and other hazardous gases [17]. Dust haze particles induced by sand storms consist of aluminum silicon oxide (AlSiO), silicon dioxide (SiO_2) and calcium carbonate ($CaCO_3$) [18]. Bushfire smoke compositions are mainly carbon oxides and nitrogen oxides [19], which are often smaller than other atmospheric particles, such as water droplets, sand, or sea salt [20]. In addition to the severe health issues caused by industrial exhausted aerosols [21], dust storms particles [22], and bushfire smoke [23], these phenomena cause significant losses in irradiance reaching the PV cells [24], spectrum changes [25, 26] and haze's particle deposition, which

* Corresponding author. Department of Electrical & Computer Engineering, Western University, ON, Canada.
E-mail address: joshua.pearce@uwo.ca (J.M. Pearce).

https://doi.org/10.1016/j.rser.2022.112796
Received 27 April 2022; Received in revised form 26 June 2022; Accepted 18 July 2022
Available online 5 August 2022

Nomenclature

Abbreviations definitions

a-Si	Amorphous silicon
a-Si:H	Hydrogenated amorphous silicon
AERONET	Aerosol robotic network
AlSiO	Aluminum silicon oxide
ANN	Artificial neural network
ARIMA	Autoregressive integrated moving average
ASTM	American Society for Testing and Materials
BP	Back propagation neural network
$CaCO_3$	Calcium carbonate
CdTe	Cadmium telluride
CERES	Clouds and Earth's Radiant Energy System
CIGS	Copper indium gallium selenide
COP	UnitedNations Climate Change Conference
c-Si	Crystalline silicon
CSP	Concentrated solar thermal power
CPV	Concentrated photovoltaic
ECMWF	European Centre for Medium-Range Weather Forecasts models
GaAs	Gallium arsenide
GBDT	Gradient boosted decision trees model
GCM	Global climate modeling
GEM	Global environmental multiscale
GISS	Goddard Institute for Space Studies
GSEE	Global Solar Energy estimator
HCPV	High-concentration PV
ICPMS	Inductively coupled mass spectrometry
IEEE	Institute of Electrical and Electronics Engineers
InN	Indium nitride
J	Junction
LCPV	Low-concentration PV
LOESS	Locally weighted scatterplot smoothing
NASA	The National Aeronautics and Space Administration
NASA's AIRS	Atmospheric Infrared Sounder on NASA's Aqua Satellite database
NASA's EOS	NASA's earth observing system
NASA's MAIAC	Multi-angle implementation of atmospheric correction
NASA's MERRA	Modern-era retrospective analysis for research and applications dataset
NASA's OMI	NASA's ozone monitoring instrument
NO_2	Nitrogen dioxide
NREL	National Renewable Energy Laboratory
NWP	Numerical weather prediction
MAIAC	Multiangle implementation of atmospheric correction
MARS	Multivariate adaptive regression splines
MPP	Maximum power point for a PV module
PAR	Photosynthetically active radiation
PCC	Pearson correlation coefficients
PM	Particulate matter
PV	Photovoltaic
SARAH	Surface solar radiation data set - Heliosat
SiO_2	Silicon dioxide
SO_2	Sulfur dioxide
SO_4	Sulfate
STC	Standard test conditions
SVR	Support vector regression
TMY	Typical meteorological year data
UV	Ultraviolet
WRF	Weather research and fore-casting models

Parameters

a_{PV}	Coefficient determined empirically that establishes the upper limit on module temperature when wind speeds are low and solar irradiance is high
AM	Air mass
AM_U	Umbral air mass
AOD	Aerosol optical depth
AOD_{550}	AOD at 550 nm
$AOD_{550,U}$	Umbral AOD at 550 nm
API	Air pollution index
AQI	Air quality index
b_{PV}	Coefficient determined empirically at which module temperature decreases as wind speed increases
CF	Capacity factor (%)
$LCOE$	Levelized cost of energy [$]
DHI	Diffuse horizontal irradiance [W/m^2]
DNI	Direct normal irradiance [W/m^2], [MJ/m^2/day]
$Ef_{PM,abs}$	PM mass absorption efficiency [m^2/g]
$Ef_{PM,scat}$	PM scattering efficiency [m^2/g]
EIR	Effective irradiance ratio (%)
$EIR_t^{I_{SC}}$	Effective irradiance ratio based on short-circuit current (%)
EIR_t^{MMF}	Effective irradiance ratio based on mismatch factor (%)
EN_{AC}	AC output energy [J]
G	Solar irradiance [W/m^2], [kWh/m^2/day]
G'	Irradiance of examined solar cell or module [W/m^2]
G_0	Measured irradiance in clean day [W/m^2]
GHI	Global horizontal irradiance [W/m^2]
$G'_{I_{SC}}$	Irradiance of examined solar cell or module calculated based on short circuit current [W/m^2]
$G_{measured}$	Measured irradiance by sensor [W/m2]
G'_{MMF}	Irradiance calculated based on mismatch factor [W/m^2]
$G_{PM2.5}$	Measured irradiance in hazy day [W/m^2]
H_{amb}	Relative humidity [g/m^3]
i	Index, represent specific element
IRR	Internal rate of return
I_{SC}	Short circuit current [A]
	Short-circuit current of AM1.5G spectrum [A]
$I_{MPP}^{Measured}$	DC-generated current of PV module [A]
$I_{SC}^{Nominal}$	Nominal I_{SC} [A]
$I_{SC}^{Real\_Spectrum}$	Short-circuit current of real world spectrum [A]
$M_{PM,T}$	visible solar energy to the total mass loading within a specified time period [g/m^2]
$M_{PM,i}$	Mass loading of component i [g/m^2]
MMF	Spectral mismatch factor
n	Number of elements in atmosphere
NPV	Net present value [$]
$nRMSE$	Normalized root mean square error
P_0	Nominal DC power of installed PV [W]
P_{AC}	Output AC power [W]
P_{max}	Maximum output power [W]
P_{out}	Output power [W]
P_{CPV}	Potential estimated CPV power output [W]
P_{PV}	Potential estimated PV power output [W]
P_{STC}	PV module power at the standard test conditions [W]
PBP	Payback period
$POAI$	Point of array irradiance [W/m^2], [kWh/m^2/day]
$POAI_0$	Point of array reference irradiance [W/m^2]
$PM\ 2.5$	Mass of particles smaller than 2.5 μm [μg/m^3]
$PM\ 10$	Mass of particles smaller than 10 μm [μg/m^3]
PR	Performance ratio (%)
PSI	Pollutant standards index
Q	Solar insolation [W/m^2],[kWh/m^2/day]
R	Coefficient of determination
r_1	Ratio of short-circuit current generated under real world spectrum ($I_{SC}^{Real\_Spectrum}$) and theoretical short-circuit current

	generated under AM1.5G spectrum ($I_{SC}^{AM1.5G}$)
r_2	Ratio of DC-generated currents of PV modules ($I_{MPP}^{Measured}$) to the short-circuit current generated under AM1.5G spectrum ($I_{SC}^{AM1.5G}$)
RMSE	Root mean square error
SR	Spectral response [A/W]
SSA	Single scattering albedo
T	Transmittance
T_{AOD}	Light transmittance affected by aerosols
T_{TPW}	Light transmittance affected by water in atmosphere
t	Time [s]
TPW	Total perceptible water
V_{OC}	Open-circuit voltage [V]
V_{wind}	Wind velocity [m/s]
Y	Energy yield [kWh/kWp]
Y_f	Final PV system yield [kWh/kWp]
Y_r	Reference yield [kWh/kWp]

Greek symbols

$_{ISC}\alpha$	The temperature coefficient related to the short-circuit current [1/°C]
α_{CPV}	Coefficient specific to CPV module [°C/Wm^{-2}]
β	Particulate matter up scatter fraction
$\Delta\theta_{cnd}$	Difference of the module temperature and the module's back surface temperature at 1000 W/m^2 irradiance level [°C]
δ_{CPV}	Cell's temperature coefficient for CPV model [1/°C]
ε_{CPV}	Air mass coefficient for CPV model
η	Conversion efficiency (%)
θ	Temperature [°C]
θ_{amb}	Ambient temperature [°C]
θ_{m}	Temperature of the module's back surface [°C]
θ_{mod}	Module's temperature [°C]
$\theta_{\text{mod}}^{avg}$	Annual module temperature [°C]
$\theta_{\text{mod}}^{STC}$	Module's temperature at STC conditions [°C]
φ_{CPV}	Aerosol optical depth coefficient for CPV model

also decrease conversion efficiency (η). Irradiance change caused by haze directly affects the power generation of PV plants (P_{out}), solar irradiance (G), insolation (Q), energy yield (Y), and conversion efficiency (η) [27]. For that reason, the first step in assessing PV power plants' production should be calculating irradiation at the PV modules and spectrum variations after being affected by the aforementioned phenomena [25, 26]. Soiling can be considered a further outcome of haze [28], severely reducing power generated by PV systems from direct shading [28, 29]. A schematic illustration of the various impacts of haze on solar energy generation is shown in Fig. 1.

Historically, PV systems were deployed in ideal environments, but as the economics of PV have improved, PV deployments have expanded to non-ideal locations, including those with substantial haze potential. As haze is such a widespread environmental concern and PV is now being deployed in these areas a review is needed to help provide clear guidance for best practices to developing PV in high-haze areas. To do this, this article provides a systematic literature review of PV electricity generation under haze and their impacts on solar cells is not yet available. This paper is structured as follows: Section 2 comprehensively describes how researchers correlate haze concentration to PV output and what materials are needed for this purpose, discussing the methodologies and approaches for analyzing the impacts of haze on PV systems. Section 3 discusses the effect of haze on the output PV power plants worldwide over the years and presents results from the literature. Finally, Section 4 discusses practical solutions for discussed problems concerning the impacts of haze on PV energy generation, and Section 5 provides conclusions highlighting significant results, and suggestions for future work.

1.1. Why haze affects PV energy generation

To optimize PV system performance in suboptimal locations, it is essential to understand the physics behind the reduced performance of PV as a result of haze. First, PM suspended in the air prevents some

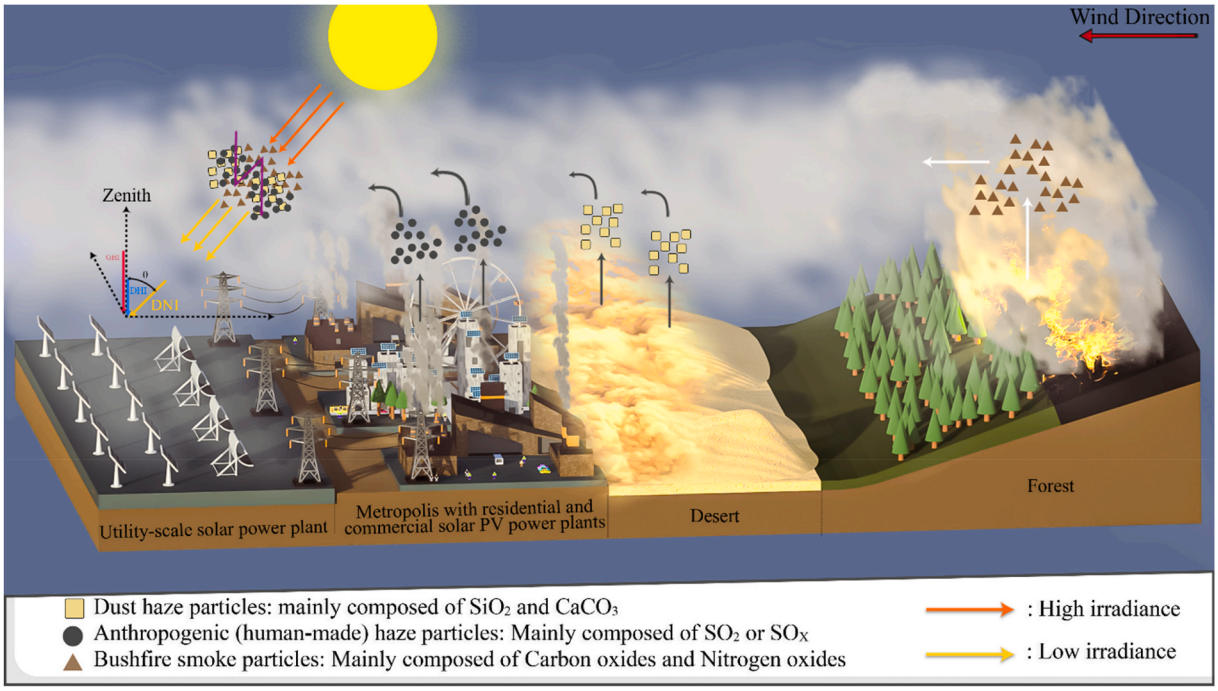

Fig.1. Schematic illustrations of the impact of haze on PV power generation.

sunlight from reaching the PV. When the concentration of PM increases, the optical depth (light transmission from the atmosphere to the Earth) is influenced, and consequently, the aerosol optical depth (*AOD*) will increase. *AOD* is the most critical parameter for analyzing the amount of solar radiation's extinction by particles in the atmosphere. An increase in *AOD* contributes to a reduction of solar energy generation through direct radiative forcing (with scattering and absorption by atmospheric PM) and indirect radiative forcing (with changing cloud albedo as well as cloud lifetime), and lowering the light transmittance (*T*) [30-32] (see Fig. 2). Numerous studies have demonstrated a decrease in short-wavelength irradiance (Fig. 3) and photosynthetically active radiation (PAR) as *AOD* increases (such as in China [33], Australia [34] and Spain [35]). As a result of the aforementioned phenomena, the spectrum and irradiance intensity will change as a result of haze (Rayleigh scattering [25]) (Fig. 3). This is the main reason behind the degradation in performance of PV systems by haze, which will be discussed in Section 1.2. Haze can also lead to other phenomena degrading the output of PV systems, such as deposition of airborne particles on PV modules (soiling) and irradiance mismatch [irradiation deviation from standard test conditions (STC)]. Soiling is out of the scope of this review, and interested readers are referred to Refs. [36-41] for reviews and comprehensive articles on this topic.

1.2. Change in spectrum and irradiance intensities

Due to sun path geometry and weather conditions, the air mass (AM) changes during the day; hence PV systems will perform differently compared to STC AM1.5 conditions (See Fig. 3). These losses are typically estimated at around 1% [44, 45]. During haze events, however, these effects are more severe, and PV systems are expected to experience more losses [26, 46]. These spectral shifting impacts will depend on the spectral response of the used PV technology [26, 46-48]. It should be noted that as the PM values increase, the intensity of the visible and UV range are greatly reduced while in the infrared intensity increases.

To quantify these impacts, the performance ratio (*PR*) (Eq. 1) is used for assessing PV system performance and is calculated by:

$$PR = \frac{Y_f}{Y_r} = \frac{\frac{EN_{AC}}{P_0}}{\sum \frac{POAI}{POAI_0}} = \frac{POAI_0}{P_0} \times \frac{\sum P_{AC}}{\sum POAI} \quad (1)$$

In Eq. 1, Y_f is the final PV system yield, Y_r is reference yield, EN_{AC} is net AC output energy, P_0 is nominal DC power of installed PV, P_{AC} is the ac power of the PV system, *POAI* is in-plane irradiance, which can be measured by a sensor at the same orientation of the PV module, and $POAI_0 = 1000$ W/m^2 is reference irradiance. Another approach to describing this phenomenon is the annual effective irradiance ratio (*EIR*), which is:

$$EIR_t = \frac{\sum_t G'}{\sum_t G} \quad (2)$$

EIR is defined as the ratio between the effective irradiance intensity of examined solar cell (G') and reference module irradiance (G) [46].

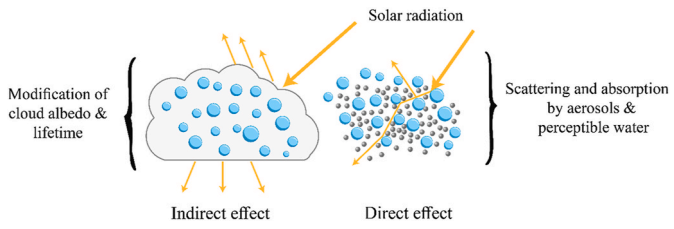

Fig.2. Radiative forcing by scattering and absorption of solar radiation, changes in clouds albedo and lifetime owing to aerosols and clouds in the atmosphere.

Consistent with the results shown in Fig. 3, Liu *et al.* [26] demonstrated that during an event of haze in Singapore in 2013, the reduction in irradiance was not uniform across the spectrum. The spectrum reaching PV modules was found to be considerably less blue-rich in the presence of haze than on a typical day [26]. They found a more significant decrease in shorter wavelengths, which is the main reason for variations in PV generation in Singapore (particularly those of high bandgap PV thin film materials such as amorphous silicon (a-Si:H), cadmium telluride (CdTe) and copper indium gallium selenide (CIGS) [26, 46]). For example, the *PR of* a-Si:H PV decreased up to 7% in hazy weather conditions [26], while there was a constant trend in *PR* for crystalline silicon (c-Si) PV. The reason behind the good performance of c-Si under hazy conditions is that they have a higher spectral response (*SR*) at near-infrared wavelengths because of their relatively low bandgap (1.12 eV). PV cell materials with a lower band-gap like c-Si, indium nitride) InN(, etc. show a *SR* peak in the infrared region, whereas those with a larger band-gap closer to the ideal of AM1.5 spectrum have a maximum *SR* at higher photon energies (See Fig. 3). Therefore, this raises an important point that higher band-gap PV technologies are more vulnerable to haze, which may play a role in location optimized PV of the future [49]. On the other hand, without haze, the a-Si module performs better in Singapore. The reason is that the spectrum in Singapore is blue-rich [46]. Likewise as haze from pollution is reduced, optimal PV selection may shift to higher bandgap semiconductors for a particular region. In addition, whendesigning and establishing power plants in regions like Singapore, which experience haze frequently, optimal optical engineering is more complicated, and more factors should be considered [26].

According to Ye *et al.* [46], haze negatively influences the performance of some solar cell technologies as scattering of short-wavelength light decreases by aerosols and particles in the atmosphere (similar to Fig. 3) [50, 51]. During an event of haze, owing to a red-shift appeared in the irradiance spectrum, the *EIR* for a-Si systems decreased by 2%, CdTe modules experienced a slight decrease in *EIR*, while copper indium gallium selenide (CIGS) and double-j (jumction) micromorph solar cells (a-Si/μc-Si) were not affected [46].

Peters et al. [42] indicated that in Delhi, perovskites modules are affected most by haze following by CdTe, gallium arsenide (GaAs), and c-Si PV modules, i.e., GaAs, CdTe, and perovskite PV modules experienced 23 %, 33 %, and 42 % more losses in comparison with c-Si, respectively, because they depend on shorter wavelength light (also indicated in Fig. 3). This impact is slightly dependent on the haze of a given city as shown in Fig. 4. Another result previously illustrated in Fig. 3 by Peters et al. [42] shows the effect of fine particles equal or smaller than 2.5 μm (PM2.5) on the spectral irradiance compared to most common PV technologies spectral responses. This strongly verifies the aforementioned outcomes regarding the variation of the spectrum and decrease in shorter wavelengths irradiance, which is also in line with Rayleigh scattering theory [25] and other research indicating that there is higher absorption at short wavelengths because of nitrated and aromatic aerosols in haze [52]. Therefore, it is clear that PV power output exposed to haze mainly depends on the material technology used, where higher bandgap materials are more vulnerable to haze.

2. HOW to correlate haze concentration to PV performance

After the spectral impacts of haze on PV are understood, it is possible to correlate PV performance to haze concentration. Different factors contribute to haze concentration and important parameters affecting and affected by haze phenomena are summarised in Fig. 5. The primary material employed in the literature to define a correlation between haze concentration and PV performance is analysing of the data obtained by meteorological tools, such as satellites data or surface-based experiments, and modeling methods.

As climatic phenomena are the primary variable with haze, meteorological tools are critical for PV research in this context. They provide

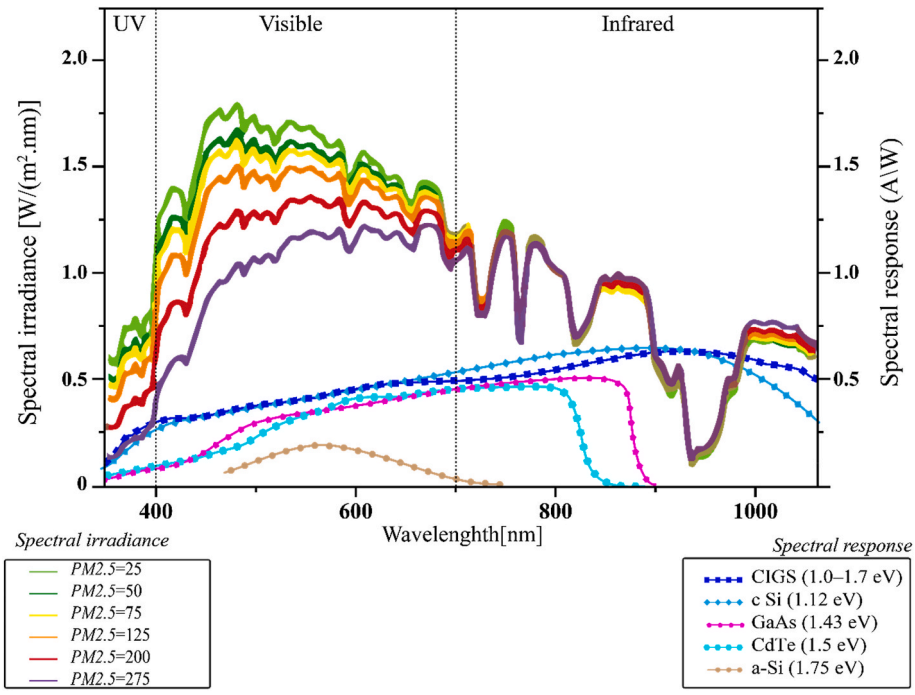

Fig.3. Spectrum changes due to *PM2.5* haze versus spectral responses of most common PV materials (data from [42, 43]).

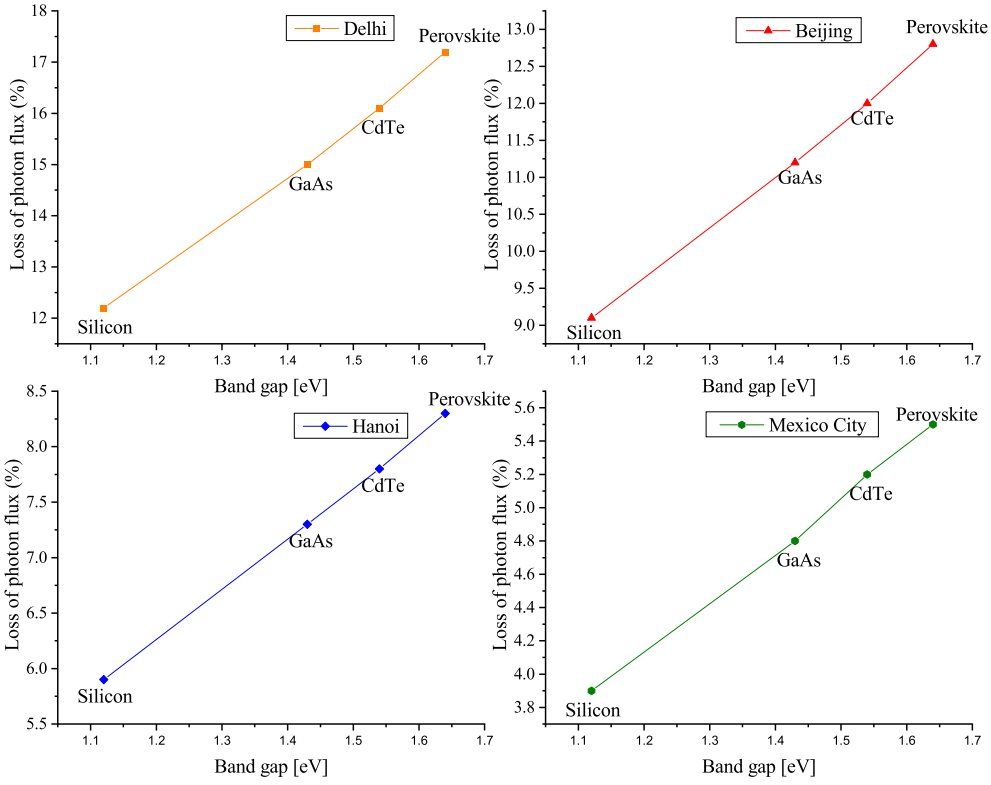

Fig. 4. Losses in photon flux absorbed by different PV technologies in different cities (adapted from data in [42]).

essential data for the establishment of analysis to estimate solar irradiance extinction. Aiding data analysis methods, and mainly for data collection purposes, outdoor experiments are also conducted as field measurements during haze events or low irradiation periods. System performance modeling methods were widely developed to focus on meteorological and PV power plant data, addressing issues of solar power generation under haze, while spectrum measurements and calculations to investigate the effects of particulate matter on spectrum changes are also used in the literature, analysing potential spectral changes and their effect on PV power generation.

Table 1 summarizes the tools, models, and methodologies utilized in the literature in this area, along with their specifications, aiding prospective researchers to employ these methods or develop new, improved methods for assessing the effect of haze on solar energy systems.

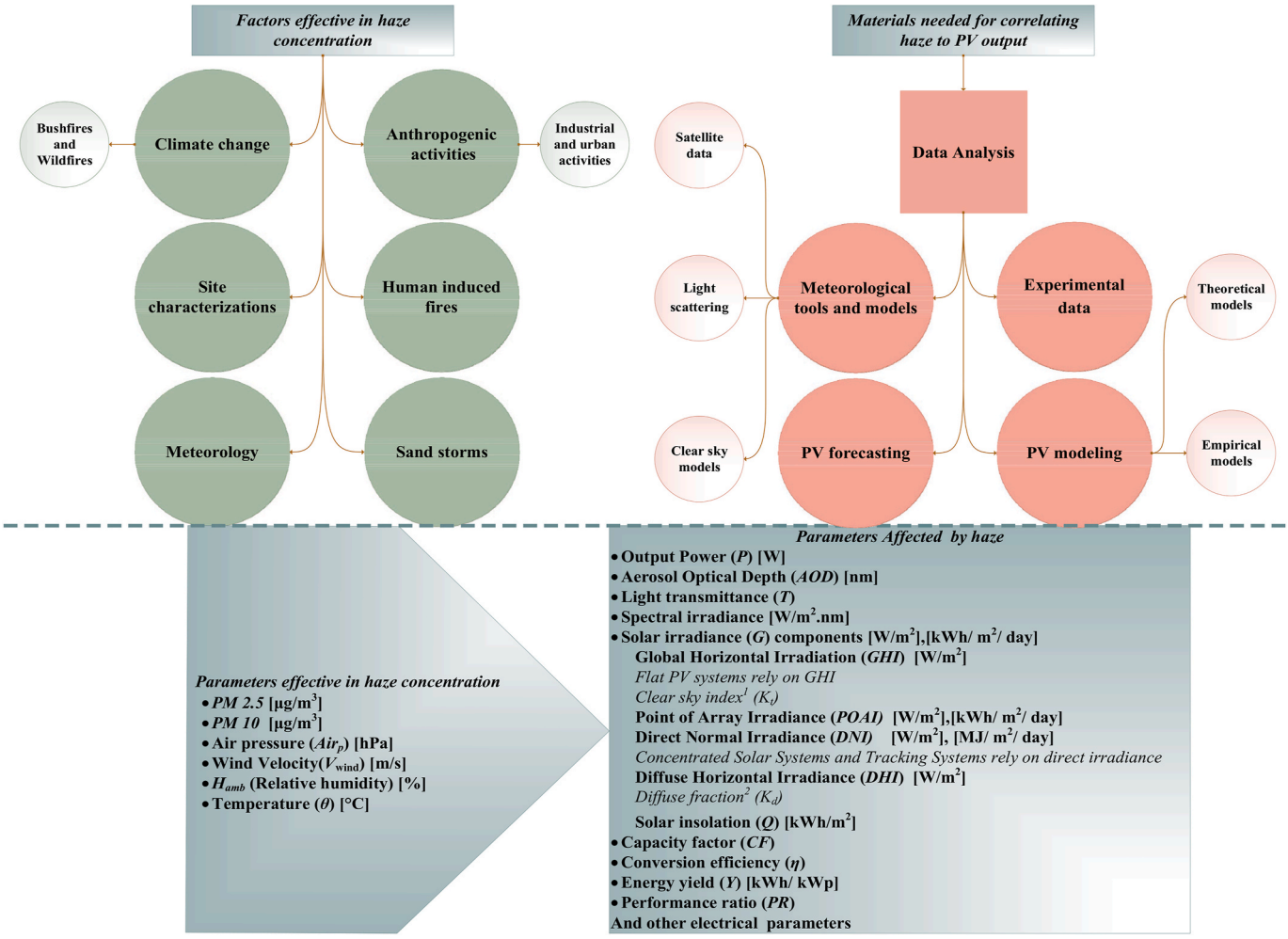

Fig.5. Main factors, parameters and materials needed for analysing haze concentration and PV energy generation under hazy weather conditions.[11,22]

Particular attention and more information are devoted in the last column of Table 1, e.g., noting if the tools are open source and can thus be more readily accessible to all researchers.

2.1. Data collecting, analysis, and modeling

2.1.1. Meteorological tools and models

2.1.1.1. Satellite data. Satellite-derived data can be employed for obtaining meteorological information such as temperature as well as irradiance data. These data can be used as input for modeling methods, and accessing them increases the speed of investigations and avoids time-consuming site measurements. Some satellite data used in the literature are listed in Table 2.

2.1.1.2. Light scattering estimation. Bergin *et al.* [55] studied the reduction induced by aerosols in light transmittance *(T)* and solar energy generation. In the first step of their research, chemical characteristics of dust were determined using inductively coupled mass spectrometry (ICPMS) [127] for identifying up to 50 elemental components and the ASTM D5373-08 method to obtain total carbon, nitrogen and hydrogen. Obtaining chemical characteristics helps researchers determine the fraction of carbon in the dust. Then, based on the modeling of PM radiative forcing proposed in the global climate modeling (GCM), losses due to PM were identified. GCM utilize Goddard Institute for Space Studies (GISS) ModelE2, which evaluates both *DNI* and *DHI*, takes into account the effects of clouds, and considers the effects of PM on the visible flux at the Earth's surface. It is noteworthy that solar PV were considered fixed and horizontal in their assessments, yet in real-world applications, the tilt angle is generally higher particularly as systems are deployed further from the equator. Modeling the impact of specific deposited particulate matters on solar energy resources was conducted based on Eq. 3,

$$\frac{\Delta T}{M_{PM,t}} = -\frac{1}{M_{PM,t}} \sum_{i=1}^{n} \left(Ef^{(i)}{}_{PM,abs} + \beta Ef^{(i)}{}_{PM,scat} \right) M_{PM,i} \quad (3)$$

where $\Delta T/M_{PM,t}$ refers to the transmittance changes (ΔT) of visible solar energy to the total mass loading within a specified time period $(M_{PM,t})$, n stands for specific PM components (Ex. n=5 stands for five different components), $M_{PM,i}$ is the mass loading of component *i*, $Ef_{PM,abs}$ and $Ef_{PM,scat}$ are PM mass absorption and scattering efficiencies respectively and β represents particulate matter up scatter fraction.

Peters and Buonassisi [59] studied the performance of PV solar cells by considering various factors affecting PV operation. In their study, various parameters influencing the light transmittance and PV systems, including water droplets and aerosols, were investigated between 2006 and 2015. Different metrological parameters and their correlations are involved in quantifying the performance of PV modules such as *Q*, temperature *(θ)*, total perceptible water *(TPW)*, and *AOD* to study the relationship between these meteorological parameters. For considering the effect of *TPW* and *AOD* on *T*, light transmittance affected by water in the atmosphere (T_{TPW}) and light transmittance affected by aerosols (T_{AOD}) were calculated according to SMARTS2 [69, 70] in cloudless

Table.1
Useful tools, methodologies and techniques for assessment of solar energy systems under haze used in the literature.

Tools	Methodology					
	Usage	Name	Target Parameters	Required Materials	Remarks	Refs.
Meteorological	Estimation of irradiance, weather data, light transmittance and *AOD*	NASA Satellite datasets	Global Horizontal Irradiance *(GHI) (GHI),* Diffuse horizontal irradiance *(DHI),* direct normal irradiance *(DNI), T, AOD,* Humidity, Temperature, *SSA*, Angstrom coefficient, Ground reflectance	GISS GCM ModelE, MAIAC, OMI, MODIS, CERES, MERRA, MERRA-2, SARAH, MERRA-T2M, AIRS, EOS	More information in Section 3.1.1.1.GISS GCM ModelE is open-source.	[24, 27, 42, 53-67]
	Estimation of irradiance	SMARTS2	Estimating solar irradiance, light extinction, and transmittance	Rayleigh scattering, aerosol extinction, and absorption by ozone, evenly mixed gases, water vapor, and NO_2	Open-source, Spectrum radiation model	[27, 59, 68-70]
	Estimating light extinction	IMPROVE algorithm and its revised version	Analysing light extinction	*PM 2.5*, and meteorological data	In the first IMPROVE algorithm, the assumption is that light absorption by gases is zero. The first algorithm is based on Rayleigh scattering, particle scattering, particle absorption. The revised IMPROVE algorithm has more accuracy with considering parameters such as sea salt effect and NO_2 light absorption impact.	[71-73]
	Identifying and evaluating meteorological elements	WRF-Chem	Model the emission, transportation, mixing, and chemical transformation of aerosols	Emission data	Used in the literature to calculate *PM 2.5* data	[74-76]
	Filtering cloudy environment, Clear sky irradiance detection	Reno and Hansen model	Clear sky irradiances	Actual irradiance datasets	✓Advantage: Detecting cloudy periods without misclassifying them as air pollution ✓Available in Python (PVLIB) ✓5-steps procedure discussed in Section **3.1.1.3**	[27, 77, 78]
		Nobre *et al.* model	Clear sky irradiances	Actual irradiance datasets	Based on three filters (defined in section in Section **3.1.1.3**): humidity filter, diffuse irradiance fraction filter and clean sky irradiance filter	[79, 80]
Data analysis and processing	Irradiance and output power Calculation	Yang *et al.* model	Calculating *DNI, GHI,* and *DHI*	Meteorological data (relative sunshine duration, surface pressure, perceptible water, global distribution of ozone thickness, global distribution of angstrom turbidity coefficient	✓Improved Angstrom–Prescott model. ✓Used by Zhou *et al.* for calculating *DNI* of CSP power plants	[81, 82]
		PVLIB	Calculating hourly clear sky irradiance (*DNI, GHI, DHI* and *POAI*), P_{out}, *PR,* and η.	Satellite irradiance and weather data (aerosol, clouds, temperature and other meteorology data)	✓Open-source, available in MATLAB and Python ✓More information can be found in Section **3.1.3.1.2**	[24, 78, 83-86]
		pvOps	Data normalizing	PV time-series data	✓Open-source, available in Python	[83, 87]
		Rojas *et al.* model	Estimating *DNI*, data quality control for irradiance dataset	Historical irradiance data	✓Boland-Ridley-Lauret (BRL) model	[27, 88]
	Predicting based on artificial intelligence (AI)	Persistence method	Irradiance and PV output forecasting	Historical irradiance data, PV data	✓Sutaible for dense cloud cover or clear sky ✓More information can be found in Section **3.1.4**	[89, 90]
		Autoregressive integrated moving average (ARIMA)	Irradiance and PV output forecasting	Historical irradiance data, PV data	✓Sutaible for irradiance data sets which have irregular paterns ✓More information can be found in Section **3.1.4**	[89, 90]
		Combination of Persistence method and ARIMA	Irradiance and PV output forecasting	Historical irradiance data, PV data	✓Leads to better and more accurate results compared to only Persistence or ARIMA, ✓Firstly proposed by Nobre	[89, 90]

(*continued on next page*)

Table.1 (*continued*)

Tools	Methodology						
	Usage		Name	Target Parameters	Required Materials	Remarks	Refs.
						et al. 2016 ✓More information can be found in section **3.1.4**	
			Artificial neural network (ANN)	Forecasting the output of PV systems under haze	PV data	✓Multi-layer ANN was used in the literature for forecasting PV output under haze ✓More information can be found in Section **3.1.4**	[91, 92]
			Support vector regression (SVR)	Forecasting the output of PV systems under haze	PV data	✓Used in the proposed literature to establish relationship between meteorological data and PV output ✓More information can be found in Section **3.1.4**	[74, 92, 93]
			CatBoost	Irradiance predicting	Historical irradiance data	✓Open-source ✓Random forest and gradient boosted decision trees (GBDT)-based method	[81, 94, 95]
			M5 model tree	Irradiance prediction	Historical irradiance data	✓Linear regression model ✓For predicting continuous numerical attributes	[81, 96]
			Perez *et al.* model	*GHI* prediction model	Meteorological data	✓Numerical weather prediction (NWP) model, averaged the global environmental multiscale (GEM), european centre for medium-range weather forecasts (ECMWF), and weather research and forecasting (WRF) models. Peforms better than sole models. ✓Used by Nobre *et al.* for generating *GHI* values	[90, 97]
			Back propagation neural network (BP)	Irradiance predicting	Historical irradiance data	✓A 3-layer machine learning method for solar irradiance prediction	[81, 98]
			Multivariate adaptive regression splines (MARS)	Irradiance predicting	Historical irradiance data	✓Based on regression analysis	[81, 99]
	Correlating parameters		locally weighted scatterplot smoothing (LOESS) and cubic smoothing splines	Spectrum mesurements	Spectrum data	✓In the literature it was used to analyse effect of spectrum variations on current generation, and compare actual and theoretical values of current. ✓Multivariate linear regression analysis. ✓More information can be found in Section **3.1.3.1.1**	[26, 71, 100, 101]
			Pearson correlation coefficient (PCC)	Verify the correlation established between parameters	PV data	✓Measuring robustness of linear correlations	[59, 91, 102]
	Experiments	Outdoor experiment	Electrical	Current and Voltage, Performance ratio (*PR*)	I-V meter, software programs, utility grade energy meters, and data logger	✓More information can be found in Section **3.1.2**	[26, 27, 103-105]
			Irradiance	Spectrum, irradiance (*GHI,DHI*, and *DNI*), and *AOD*	Spectroradiometer, Pyranometer, Pyrheliometer, Sun photometer and AERONET	✓More information can be found in Section **3.1.2**	[26, 27, 106]
		Indoor experiment	Chemical	Chemical characteristics of aerosols	Inductively coupled mass spectrometry (ICPMS) instrument, and ASTM D5373-08 method	✓ICPMS for elemental components analyses, and ✓ASTM D5373-08 method was conducted to identify share of total carbon, nitrogen and hydrogen	[55]
PV models and analysis	Performance and output modeling		Sandia PV Array Performance Model (SAPM)	Calculate PV DC output	Satellite irradiance and weather data	✓Used in PVLIB	[107]
					PV DC output	✓Used in PVLIB	[108]

(*continued on next page*)

Table.1 (*continued*)

Tools	Methodology					
	Usage	Name	Target Parameters	Required Materials	Remarks	Refs.
		Sandia Performance Model for Grid Connected Photovoltaic Inverters	Convert PV DC power to AC			
		NREL model	Power output	*POAI* and temperature	✓More information can be found in Section **3.1.3.1.2**	[27, 109]
		Global Solar Energy Estimator (GSEE)	Power output, *CF*	Irradiance hourly datasets	✓Open-source, its software tool is available in renewable.ninja ✓More information can be found in Section **3.1.3.1.2**	[62, 110, 111]
		MATLAB Simulink	Power output	Irradiance and temperature data	✓Firstly proposed by *Wu et al.* ✓More information can be found in Section **3.1.3.1.2**	[112]
	POAI calculation	PVLIB	*POAI*	Satellite irradiance and weather data (aerosol, clouds, temperature and other meteorology data)	✓Li *et al.* used PVLIB for calculating *POAI* ✓More information can be found in Section **3.1.3.1.2**	[24]
		Khoo *et al.* model	*POAI*	Satellite irradiance	✓Used by Nobre *et al.* for calculating *POAI*	[89, 113]
		Isotropic-sky insolation	Estimating *POAI*	Irradiance datasets	✓Appropriate for overcast days	[114, 115]
		Anisotropic-all-sky model	Estimating *POAI*	Irradiance datasets	✓Appropriate for clear days	[115, 116]
		Enhanced anisotropic-all-sky model	Estimating *POAI*	Irradiance datasets	✓Proposed by Klucher ✓Appropriate for both overcast days and clear days	[115]
	CPV performance and output modeling	Fernández *et al.* model	Potential power output	*AM*, *AOD*, temperature, *DNI* data	✓Mathematical modeling of CPV potential spectral distribution and the electrical output ✓More information can be found in Section **3.1.3.1.2**	[27, 117, 118]

Table.2
Satellite-derived data used in the literature for experimenting haze impacts on PV.

Dataset name	Application in evaluating haze	Availability	Literature Reference
NASA'S MAIAC	*AOD* estimations,	Data freely available on [119]	[27, 53]
NASA's OMI with NASA's MODIS	*AOD*, single scattering albedo (*SSA*), Angstrom coefficient, ground reflectance estimations	NASA's OMI is available with registration [57, 120], MODIS data is freely available [58], MODIS script freely available [58]	[59]
GISS GCM ModelE	Light transmittance estimations,	Code freely available on [56, 121]	[55]
CERES	Irradiance estimations	Data freely available through [60, 122]	[24, 42, 59]
MERRA	Irradiance estimations	Free access on [123]	[61, 62]
MERRA-2	Irradiance estimations	Free access on [124]	[62, 63]
SARAH	Irradiance estimations	Data available through [125]	[62, 64]
MERRA-T2M	Temperature data Used to estimate of θ_{amb}	Free access on [124]	[62]
NASA's AIRS and EOS	Relative surface humidity and total perceptible water data	Data available through [65, 126]	[59]

[1] Ratio of observed GHI to the estimated GHI under clear sky conditions, both at ground level.
[2] Ratio of DHI to the GHI.

conditions. In the Del Hoyo *et al.* study [27], a sun photometer with Aerosol Robotic Network (AERONET) was employed to obtain *AOD* values [27]. For this purpose, they used Multi-Angle Implementation of Atmospheric Correction (MAIAC) AOD by NASA, which employ satellites data from Moderate Resolution Imaging Spectroradiometer (MODIS) AQUA and NASA'S TERRA projects. The MAIAC consist of *AOD* values at 470 nm, 550 nm and water vapor data at spatial resolution of 1 km.

2.1.1.3. Clear sky modeling. Obtaining clear sky irradiance is necessary for assessments, as these values are compared to hazy days' irradiance values. In the context of the effect of haze on PV energy systems, two efficient clear sky identification procedures were used, which are described here. For future research, new clear sky models such as [128-133], and their results in investigating haze can be compared and discussed [134]. A strong clean sky detection model was proposed by Reno and Hansen [77], and this method was used by Del Hoyo *et al.* [27] to reach clear sky irradiances. In the first step, days with *GHI* considerably below the mean value are classified as cloudy. The next criterion examines the maximum of *GHI* to discover periods when the *GHI* rises due to brightness induced by clouds, and then compare it with the clear sky model value. The third criterion compares the variation of a clear sky model compared to the variation of a time period. The fourth one investigates the maximum difference between *GHI* and the calculated irradiance by a clear sky model. The final criterion determines the standard deviation of *GHI* variations; defining periods as overcast if it exceeds 8W/m^2. This model is available in the open source Python community-supported tool [27, 77, 78].

Moreover, a methodology based on three filters to obtain irradiance values on clear sky days (pollutant standards index *(PSI)*<50) was proposed by Nobre *et al.* [79] to study the effect of haze on PV

technology. These values are considered baseline days without haze. These clear sky days are identified by statistical analysis of recorded data. The humidity filter (as the first filter) is used to discard conditions with a relative humidity greater than 80%, which are related with rain or cloudy pre/post rainy conditions. After applying a humidity filter, a diffuse irradiance fraction filter is employed on all the data, which passed the previous filter to eliminate situations with diffuse irradiance fraction ratio (K_d) above 0.5 (high cloud cover and no rain). Finally, clean sky irradiance band filters were utilized to complete the above-mentioned filters by omitting previously verified irradiances that are not within a range of ±100 W/m^2 clear sky values, defined by model [80] (circumstances with cloud enhancement effects). The arbitrary threshold of 100 W/m^2 was chosen to consider more verified values, yet strict enough to delete points that are clearly outside the proposed range of the clear sky model.

2.1.2. Experimental data

If proposed data are not available by satellites or more accurate data are needed, site measurements and experiments can be employed. Conducting field measurements, local experiments, and systems monitoring are needed to validate the haze models and theories and prepare the basis for future developments. Zagouras *et al.* [135] pointed to distributing ground sensing networks for optimal irradiance measuring. The meteorological network in Singapore employed by Nobre *et al.* [79, 89] is an excellent example of these sensing networks, in which several stations (8 peripheral stations + 1 validation station) were used for data collection and validation during an haze observations in Singapore. Table 3 lists some instruments used by researchers in the literature to measure parameters affected by haze.

There have been several experimental studies quantifying the PV energy loss due to haze. For example, Maghami *et al.* [103] studied the effect of air pollution particles on the power generation of fixed and tracking flat PV. Local weather stations recorded various meteorological parameters and P_{out} and Y were measured to obtain a relation between haze and solar power generation. Finally, multiple regression analysis [136] was used to confirm the correlation between meteorological parameters and power generation losses. Maghami *et al.* [103] showed that fixed flat PV arrays are more suitable than the tracking flat PV array in a country like Malaysia with a tropical environment that experiences haze events frequently.

In 2017, Abd Rahim *et al.* [105] carried out outdoor electrical experiments and economic analysis to assess the impact of bushfire smoke on PV performance in Malaysia. They measured the P_{max} of a PV panel, irradiance (G), and module temperature (θ_{mod}) for two periods of hazy and clean sky conditions to quantify production losses in PV modules. They [105] reported 17.8 % decrease in PV module power output during a haze event. Based on economic analysis [105], an 8 % reduction in net present value (*NPV*), and a slight decrease in internal rate of return (*IRR*) were reported, while the payback period (*PBP*) increased around 10 % when haze was present in Malaysia for 6 months. Lastly, to determine the relationship between PV output and haze induced by wildfire, they used analysis of variance (ANOVA), which resulted in R square value of 0.991921 [137]. In terms of electrical parameters, this study only discussed I, V and P_{max}., but future work could also evaluate the fill factor (*FF*). Recently, Chen *et al.* [106] studied the negative effects of haze on PV panels installed in Shanghai, China. In this study, the *PM2.5* concentration was recorded over a period of one year via an online local air quality system. Then, three months with the highest haze level were selected, and G was recorded for these months by a pyranometer. Finally, the correlation between haze, irradiance, and consequently, power generation of PV was investigated based on well-described methodologies [42, 79] to compare experimental results with estimated values. Chen *et al.* [106] showed that *PM2.5* and G were inversely correlated. For *PM2.5* concentration of 73 μg/m^3, the irradiance and power generation reduction percentages were 38.6% and 39.7%, respectively (46.9% irradiance reduction and 49.6% power reduction for 105 μg/m^3). Their financial analysis showed that the payback periods with and without air pollution were 6.64 and 6.12 years, respectively.

Table 3
Laboratory instruments used in the literature for experimental measurements of haze impacts on solar PV.

Equipment	Application in examining haze	Ref.
Spectroradiometer	Spectrum measurement	[26, 106]
Pyranometer, silicon sensor	Measuring *GHI* and *DHI*	[26, 27, 79, 89, 106]
Pyrheliometer	Measuring *DNI*	[27]
Two-axis sun tracker	Sun tracking for irradiance measurements	[27]
Automatic sun photometer	Measuring *AOD*, Angstrom coefficient, *SSA*, Asymmetry factor, concentration of aerosols and water vapor data	[27]
Ultrasonic anemometer	Measuring V_{wind} (wind velocity)	[27]
ICPMS instrument	For elemental components analyses	[55]
I-V meter, Shunt/ transducer	Measuring cells current and voltage	[26, 27, 79, 89, 103-105]
Energy meter	Measuring power and performance ratio	[26, 79, 89]
Datalogger	For saving measured data	[27, 103-105]

A closer look at the literature on the impact of haze on PV systems reveals several gaps and shortcomings, especially related to controlled indoor experiments. Conducting indoor experiments, for example, at laboratories with a dust chambers and solar simulators (particularly those with both intensity and spectral control), would be beneficial for establishing empirical linear and non-linear relationships between haze concentration and losses in PV power output. An extensive framework for future studies based on experimental studies and current research gaps in the literature is shown in Fig. 6 to demonstrate the outdoor and indoor electrical experiment procedures and compare the results with modeling methods.

2.1.3. PV Modeling

2.1.3.1. Theoretical modeling. A large number of theoretical or physical-based models are available in the literature for analysing the relationship between haze and PV energy degradation, such as Sandia PV Array Performance Model (SAPM) to calculate PV DC output [107] and Performance Model for Grid-Connected Photovoltaic Inverters to calculate PV AC output [108], both implemented in the open source pvlib and open source SAM [138]. The NREL equation [109] was used by Del Hoyo *et al.* [27] for potential estimated PV power output (P_{PV}) estimation on hazy days (Eq. 11). These types of models can be employed for different locations and applications. In the following sections, the most appropriate physical models for investigating the effect of haze on PV systems are discussed.

2.1.3.1.1. Spectrum modeling. A novel spectral analysis was performed by Liu *et al.* [26]. They gathered data from PV power plants in Singapore for precise analysis and modeling to evaluate the impact of haze on the spectrum and solar irradiance. Therefore, r_1 and r_2 ratios are defined as follows:

$$r_1 = \frac{I_{SC}^{Real\_Spectrum}}{I_{SC}^{AM1.5G}} \tag{4}$$

$$I_{SC}^{AM1.5G} = \frac{I_{SC}^{Nominal}}{1000} \times G_{measured} \tag{5}$$

$$r_2 = \frac{I_{MPP}^{Measured}}{I_{SC}^{AM1.5G}} \tag{6}$$

These are novel metrics for evaluating PV performance under haze at

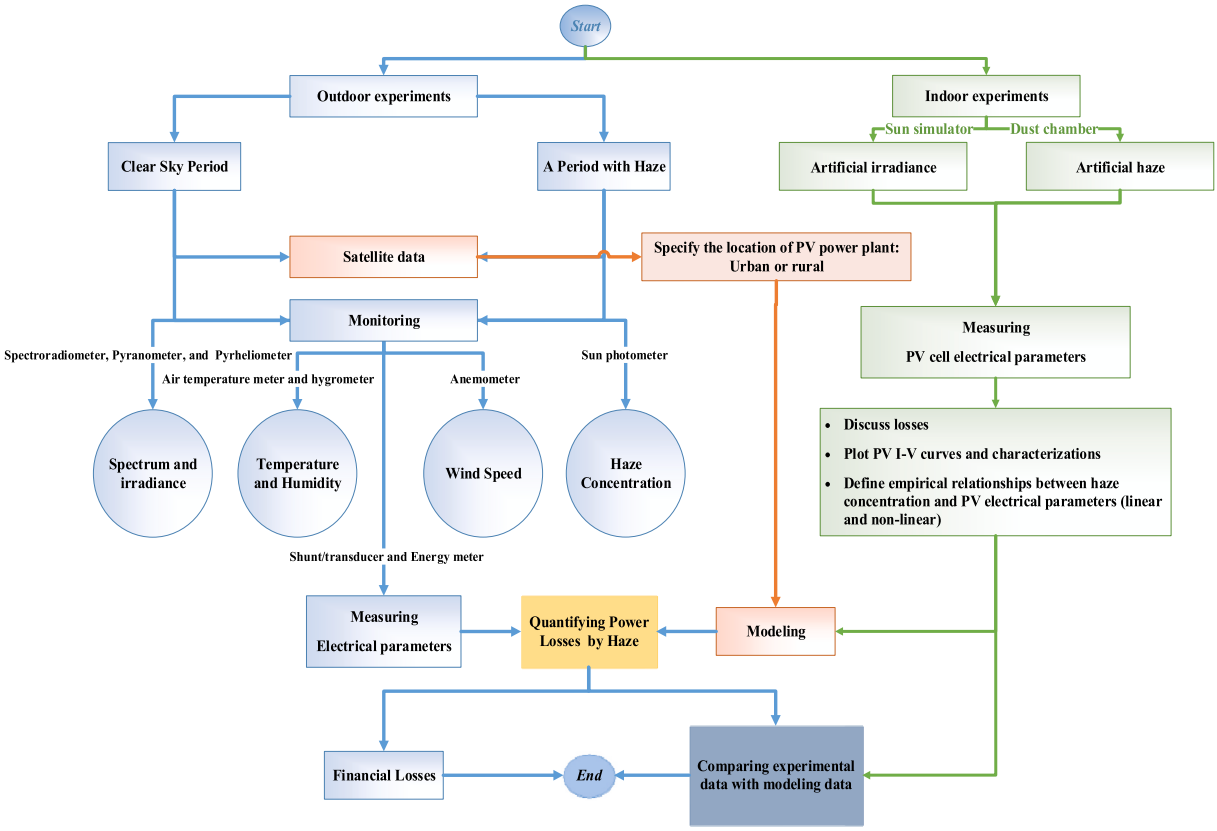

Fig. 6. A framework for outdoor and indoor electrical experiments.

the same time points. Statistical analysis [100] was established by to simply compare r_1 and r_2, where r_1 (Eq. 4) is short-circuit current generated under real world spectrum ($I_{SC}^{Real\_Spectrum}$) divided by theoretical short-circuit current generated under AM1.5G spectrum ($I_{SC}^{AM1.5G}$, calculated by Eq. 5, where $I_{SC}^{Nominal}$ is nominal I_{SC} specified on modules specification sheet and $G_{measured}$ is the measured irradiance by sensor). Moreover, they measured DC-generated currents of PV modules ($I_{MPP}^{Measured}$) and the irradiance induced on the modules, then the r_2 ratio was defined in (Eq. 6). Their two statistical analyses to establish the correlation between r_1 and r_2 were locally weighted scatterplot smoothing (LOESS) and cubic smoothing spline with ten knots, both integrated with Pearson correlation coefficient (PCC) to validate the correlation between parameters.

At the same time, Ye *et al.* [46] analysed the solar spectrum and its effect on the efficiency of PV modules by considering various technologies, including single-j a-Si, CdTe, CIGS, and double-j micromorph Si (a-Si/μc-Si). Two different approaches, including spectral mismatch factor (*MMF*) [139] and the short-circuit current (I_{sc}), were used to measure the *EIR* (Eq.2) of these four PV technologies at a function of time (t). The former is based on the *MMF* determined from the spectrum at outdoor conditions and the modules' indoor spectral responses (*SRs*). The spectral *MMF* can adapt the irradiance intensity of a test device receiving a non-standard spectrum with irradiance intensity needed under the standard spectrum. In contrast, standard test devices deliver the same current under both irradiance levels. The *EIR* based on *MMF* (EIR_t^{MMF}) is calculated based on Eq. 7, which $G_{MMF}^{'}$ can be calculated from Eq. 8.

$$EIR_t^{MMF} = \frac{\sum_t G_{MMF}^{'}}{\sum_t G} \tag{7}$$

$$G_{MMF}^{'} = MMF \times G \tag{8}$$

The latter method established on the modules' I_{SC} is measured in outdoor conditions. The irradiance spectrum's divergence from the standard spectrum affects the module's I_{SC}. Hence, the I_{SC} loss or gain compared to AM1.5G radiation reveals how the non-standard spectrum's effective irradiance intensity differs from the AM1.5G spectrum. The *EIR* based on I_{SC} ($EIR_t^{I_{SC}}$) is calculated based on Eq. 9, in which $G^{'}{}_{I_{SC}}$ can be calculated from Eq. 10. $\theta_{\mathrm{mod}}{}^{STC}$ and I_{SC}^{STC} denote module temperature and short-circuit currents at STC, G^{STC} is the irradiance with the AM1.5G spectrum,θ_{mod} is module's temperature, and $\alpha_{\ ISC}$ is the temperature coefficient for the short-circuit current.

$$EIR_t^{I_{SC}} = \frac{\sum_t G^{'}{}_{I_{SC}}}{\sum_t G} \tag{9}$$

$$G^{'}{}_{I_{SC}} = \frac{I_{SC}\left(G, \theta^{STC}\right)}{I_{SC}^{STC}} \times G^{STC} = \frac{I_{SC}}{I_{SC}^{STC}} \times \frac{\left(1+\alpha\left(\theta_{\mathrm{mod}} - \theta_{\mathrm{mod}}^{STC}\right)\right)}{} \times G^{STC} \tag{10}$$

2.1.3.1.2. Power output modeling. The pvlib-Python model flowchart is presented in Fig. 7 [84, 85] and was utilized by Li *et al.* [24] to calculate the *POAI* induced on PV modules. pvlib [78, 84-86] is an open-source MATLAB and Python based tool for simulating performance of PV systems. Researchers used this tool for calculating *POAI* [24] and hourly clear sky irradiance (GHI_{cs}, DNI_{cs}, and DHI_{cs}) [83]. Input data for the pvlib model are irradiance and weather data. The latest release of this software can be accessed through [140, 141]. The models used in pvlib are Sandia PV Array Performance Model (SAPM) [107] and Performance Model for Grid-Connected Photovoltaic Inverters [108]. Li *et al.* [24] derived surface irradiance data (period of 2003-2014 in China) from CERES [142, 143] and investigated the impact of fixed tilt angles and tracking PV systems in their research.

Sweerts *et al.* [110] presented a fully justified methodology based on

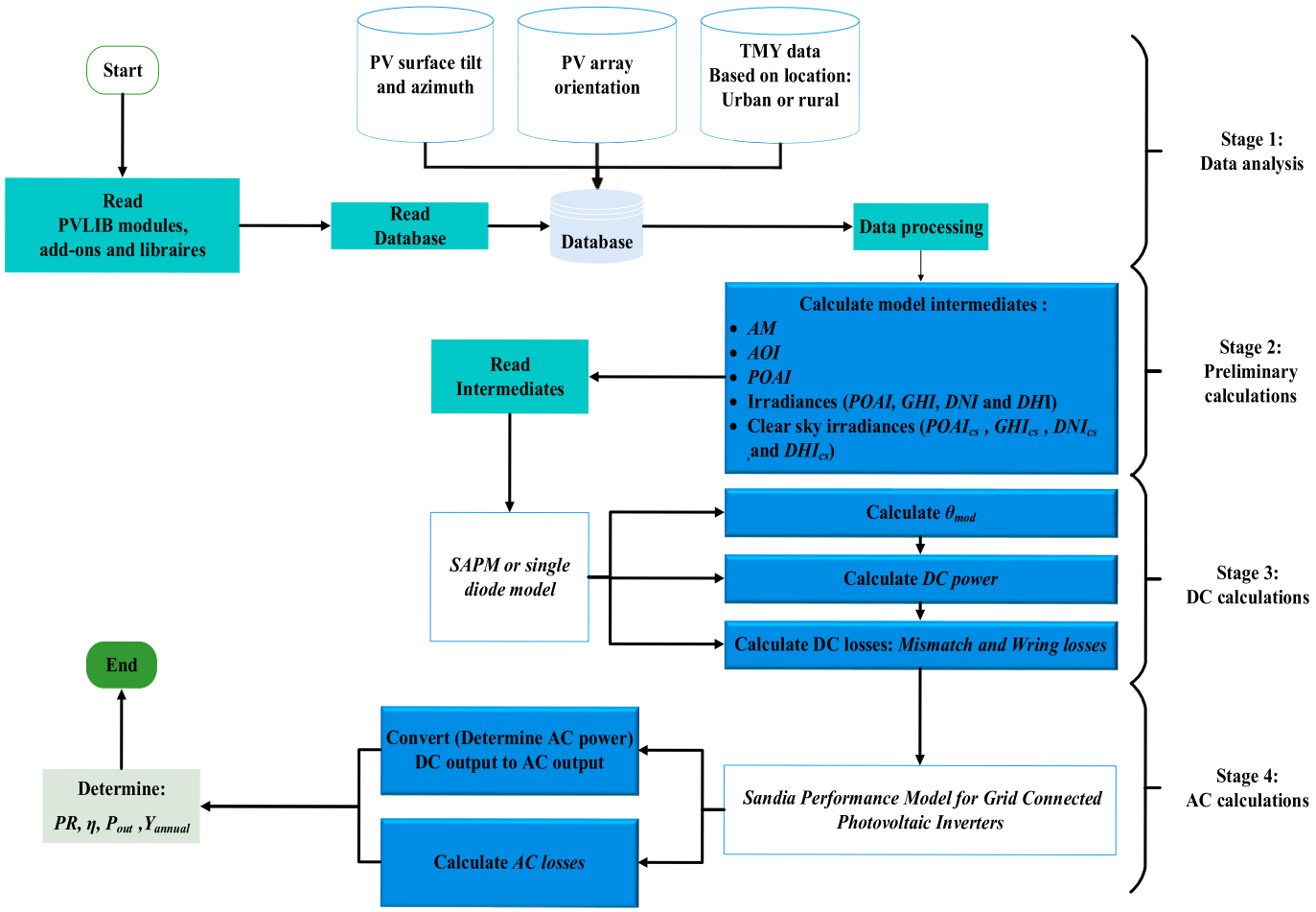

Fig. 7. Flowchart of PVLIB.

the Global Solar Energy Estimator (GSEE) [62] open-source model implemented in renewable.ninja [144]. GSEE [62] is a Python-based model, which converts hourly irradiance data into hourly power output. The flowchart of this model is presented in Fig. 8. The latest version of GSEE can be accessed through the following references [111, 145]. Radiation datasets from 1960 to 2015 in the mainland of China were utilized [110] to compute *CF* of residential PV systems and utility-scale PV power plants. *CF* is the actual generation of PV system divided by the maximum generation of PV system under laboratory conditions. Also, in their modeling, different panel orientations were considered.

In 2020, Del Hoyo et al. [21] conducted a comprehensive site-specific study in Santiago de Chile. They collected metrological data using some field measurements from 2014 to 2016 from two university campuses. Then, PV output monitoring was conducted at one campus using two different types of modules: mono c-Si and thin film a-Si. In the next step, modeling methods were utilized, in which the algorithm of Reno *et al.* [77] was employed for filtering out cloudy periods. To obtain *AOD* values and compare *AOD* loads in different locations, the MAIAC developed by NASA [53] was used. SMARTS2 model [68] was also utilized for investigating clear sky irradiance. Finally, for calculating the aforementioned PV technologies outputs, Klucher [115] model and NREL [109] (Eq. 11) were used.

$$P_{PV} = P_{STC}\left(\frac{POAI}{POAI_0}\right)\left(1 - \frac{\delta_{PV}}{100}\left(\theta_{\mathrm{mod}}^{avg} - \theta_{\mathrm{mod}}\right)\right) \tag{11}$$

where P_{PV} is the potential panel output, P_{STC} is the power at STC, *POAI* is the irradiance incident on the solar module, $POAI_0$ stands for reference irradiance, δ_{PV} stands for the temperature coefficient of power, and $\theta_{\mathrm{mod}}^{avg}$ - θ_{mod} defined as differences of annual average and operating module temperatures. To calculate θ_{mod} for flat PV modules, equation (Eq. 12) by King *et al.* [146] should be used:

$$\theta_{\mathrm{mod}} = \theta_m + \frac{POAI}{POAI_0} \times \Delta\theta_{cnd} \tag{12}$$

$$\theta_m = POAI \times \left\{e^{(a_{PV} + b_{PV} \times V_{wind})}\right\} + \theta_{amb} \tag{13}$$

where θ_{m} is the temperature of the module's back surface and can be calculated from Eq. 13, $\Delta\theta_{cnd}$ is the temperature differential between the module temperature and the module's back surface at a 1000 W/m^2 irradiance level, a_{PV} is the coefficient determined empirically that establishes the upper limit on module temperature when wind speeds are low and solar irradiance is high, b_{PV} is the coefficient determined empirically at which module temperature decreases as wind speed increases, and V_{wind} is wind velocity at a height of 10m, and θ_{amb} is the ambient temperature. At the same time, Fernandez *et al.* [117] equation (Eq. 14) was employed for simulating high concentrator photovoltaic (HCPV) potential power output (P_{CPV}),

$$P_{CPV} = \frac{P_{STC}}{DNI_{STC}} \times \left(1 - \delta_{CPV}\left(\theta_{\mathrm{mod}} - \theta_{\mathrm{mod}}^{STC}\right)\right) \times \left(1 - \varepsilon_{CPV}(AM - AM_u)\right) \times \left(1 - \varphi_{CPV}\left(AOD_{550} - AOD_{550,u}\right)\right) \tag{14}$$

$$\theta_{\mathrm{mod}} = \theta_{amb} + \alpha_{CPV} \times DNI + \beta_{CPV} \times V_{wind} \tag{15}$$

where DNI_{STC} is direct normal irradiance at STC conditions, δ_{CPV} is the cell temperature coefficient, $\theta_{\mathrm{mod}}^{STC}$ is the cell's temperature at STC

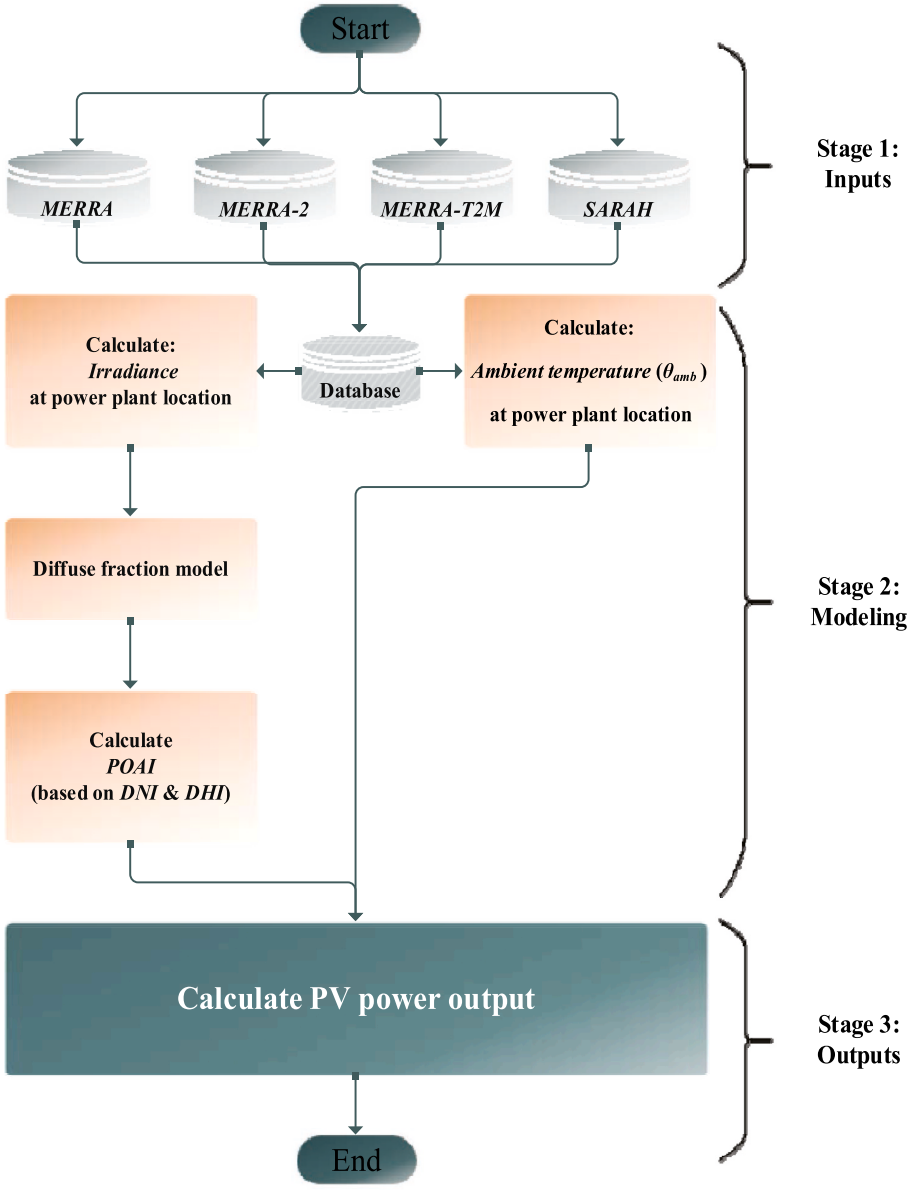

Fig. 8. Flowchart of GSEE.

conditions, ε_{CPV} is the air mass coefficient, *AM* is defined as the air mass, AM_U is defined as the umbral air mass, φ_{CPV} is the AOD coefficient, AOD_{550} is defined as the *AOD* at 550 nm and $AOD_{550,U}$ is described as the umbral AOD at 550 nm. To calculate θ_{mod} for CPV modules, Eq. 15 [147, 148] should be used, in which V_{wind} is the wind speed, and α_{CPV} and β_{CPV} are the coefficients specific to CPV module, which should be obtained empirically. In 2020, Wu *et al.* [112] used quantitative methods to quantify the effect of haze on PV modules in China. Their analysis was conducted based on data samples of PV power plants in Hangzhou and Tianjin in China. To identify irradiance changes caused by haze, they used the exponential-linear model [149], [150].

2.1.3.2. Empirical models. Empirical models are one of the tools proposed in the literature to evaluate the impact of PM on irradiance. These models were developed based on experimental results and statistical analysis. For instance, Peter *et al.* [42] derived an empirical equation (Eq.16) for calculating irradiance on hazy days. This equation was used by Chen *et al.* [106] as well to estimate irradiance in China. Similarly, Wu *et al.* [112] proposed some experimental equations for China to calculate irradiance based on *PM2.5*. Son *et al.* [151] presented some empirical equations for South Korea, correlating PV power generation to *DNI*, temperature, *PM2.5*, *PM 10*, and relative humidity. Still, indoor or outdoor experiments can derive more empirical equations for different locations and applications.

Peters *et al.* [42] conducted field measurements in Delhi to obtain PM 2.5 to define the empirical correlation between irradiance loss and PM concentrations. Furthermore, they collected data from various online sources [152-156] to project losses in other locations. Their methodology for correlating *PM 2.5* and loss in irradiation exposure is based on Ref [79], by which Peters *et al.* [42] presented empirical Eq. 16 based on their analyses. Chen *et al.* [106] and Nocerino *et al.* [157] used Eq. 16 as well.

$$\frac{G_{PM2.5}}{G_0} = \exp\left(\frac{-PM2.5}{750 \pm 90}\right) \text{Delhi, India} \tag{16}$$

$$\frac{G_{PM2.5}}{G_0} = \exp\left(\frac{-PM2.5}{250}\right) \text{Naples, Italy} \tag{17}$$

In Eq. 16 & 17, $G_{PM2.5}$ and G_0 represent measured irradiance during a hazy day and clean day, respectively, and *PM2.5* is the concentration of

particles smaller than 2.5 μm. However, Peters *et al.* [42] note that Eq. 16 is only valid for Delhi, and more studies are needed to investigate how Eq. 16 need to be adapted for other locations. Using the aforementioned methodology, firstly, they calculated relative losses in insolation using field measurements, modeling, and estimations. Then, using obtained relative values integrated with *POAI*, and PV panels power potential data [158], they estimated the loss in PV modules with an optimal angle.

2.2. Forecasting

The increasing demand for PV power worldwide will require both *short-term* and *long-term* forecasting to provide practical guidelines facilitating increasing PV deployment velocity. Therefore, forecasting the PV power plants' output operating under a hazy environment can be considered an important area of research. Different methodologies for forecasting the impact of haze on solar power generation can be employed like persistence [159] and ARIMA [160] deployed by Nobre *et al.* [89], artificial neural network (ANN) by Junhyuk *et al.* [91], and SVR machine learning by Wenjie *et al.* [74].

In 2015, seminal contributions were made by Nobre [90] in the assessment of haze on PV forecasting by combining the persistence [159] and ARIMA [160] models. Persistence is one of the simplest methods relying on time-series data for forecasting when data patterns vary slightly. While having more flexibility than persistence in handling different time series patterns, ARIMA is one the most powerful models for forecasting future values of a variable based on univariate past values of time series (auto-regression model) and past forecast errors in a regression-like model (moving average model). It is noted that ARIMA forecasting performs best in situations with irregular irradiance patterns, whereas persistence forecasting performs better in conditions of dense cloud cover or clear sky. The hybrid algorithm chooses the optimal solution adaptively and hierarchically depending on both persistence and ARIMA. In subsequent work, Nobre *et al.* [89] studied the performance of PV modules in the tropical and highly dense environment of Singapore. The architecture of this study based on Nobre's Thesis [90] is presented in Fig. 9, which would be practical for researchers to develop this subject in their regions of interest with specific PV technologies. Various factors, including PV structure, temperature, shading, long-term degradation, and pollution concentration, were considered to model *short-term* solar forecasting of reliable PV power generation. Also, the Perez model [97] was employed for short-term irradiance forecasting and generating *POAI*. In this study, persistence (yearly average *normalized RMSE* in this study is 30.8%) and ARIMA (yearly average *nRMSE:30%)* [160] forecasting were proposed for determining future changes in PV power conversion. Finally, the model was tested using a hybrid ARIMA-persistence forecast approach (yearly average *nRMSE:29%)* by considering various factors recorded using a meteorological sensing network in the understudied area. Their results showed that an integrated method containing a climate measuring system and a storm alarm system (based on ambient humidity and air pressure) can provide better results with the lowest errors. Moreover, the results of the *nRMSE* showed that the integrated method is more reliable than the persistence and ARIMA methods separately.

In recent years, in the light of *short-term* forecasting and data science methods, a feed-forward-multi-layer ANN [92] was employed by Junhyuk *et al.* [91] to forecast the output of PV power plants considering PM parameters. PCC analysis was applied to meteorological data to verify correlations between output and PM. The input layers in their model are irradiance, weather data, PM concentration, measured PV power generation in the past. They managed to improve the accuracy of PV power generation by developing some models. Furthermore, a machine learning support vector regression (SVR) algorithm [92, 93] utilized by Liu *et al.* [74] to establish a direct link between climatic variables and PV output, thereby improving the precision of PV generation. SVR is based on support vector machine (SVM) concepts, which is best suitable for linear data. To analyse meteorological elements and calculate PM concentration values, the weather research and forecasting coupled with chemistry (WRF-CHEM) [75, 76] was employed as well. Their proposed forecasting model is shown in Fig. 10. Their results indicated that the suggested method could significantly enhance the accuracy of PV power forecasting under haze, consequently assisting the dispatch and operation of the power grid.

Although preliminary works have been done to forecast future implications of haze on PV power generation, more comprehensive research should be conducted on different AI methodologies, especially in the area of "*long-term forecasting*" to prepare appropriate tools, plans, and strategies for solar energy investors and stack holders predicting the impact of aerosol on their future projects. For future studies, advanced ANN methods can be developed for accurate forecasting, such as multilayer perceptron (MLP) models [161]. Of particular interest is to investigate the impacts of future PV penetration on a haze positive feedback loop. As more PV is deployed to offset coal and natural gas-fired power plants [162, 163], as PV-powered heat pumps offset natural gas furnaces [164-167] and as PV is used for smart charging of electric vehicles that displace gasoline and deisel vehicles [168-172], PV perfromance would be expected to increase based on redution in haze from these sources. This would improve the PV system economic performance and thus accelerate the replacement of polluting fossil-fuel sources of energy with more solar PV. It is worth noticing that the studies in this context are limited to PV technology. Further investigations can also be conducted on other solar energy technologies such as low-concentration PV (LCPV) [173-177], high-concentration PV (HCPV) or concentrated solar power (CSP) [117, 118, 147, 148].

3. Worldwide effects of haze on the output OF PV systems

3.1. Geographical-associated haze

Some countries naturally experience haze owing to their specific geographic characteristics. Others are caused by human activity. For example, Singapore [79, 89], Malaysia [40, 105], Australia [15], Canada [16] and the U.S. [83]. suffer from bushfire smoke resulting from human-made forest fires or agricultural burns. China [24, 71, 110, 112] and India [42, 55, 178] are undergoing urban haze due to pollution from high population densities and intense rates of industrialization with limited emission regulations and controls. There are reports regarding bushfire haze and urban effects on PV systems in these countries. Nobre *et al.* [79] evaluated the effects of haze on the efficiency of PV modules in Singapore [79], which indicated that *GHI* levels decreased by 15% during a June 2013 haze occurrence. While the θ_{amb} was marginally higher during haze periods than on clear sky days, module temperature was lower, most likely due to a reduction in direct irradiance reaching the module surfaces.

Solar energy is typically considered to be approximately constant over long periods. However, there is clear evidence for significant multidecadal changes, called 'global dimming and brightening', because of variations in cloud features and aerosol concentrations in the atmosphere [179, 180]. Rising anthropogenic aerosol emissions are a major source of significant dimming in fast-growing and polluted places like China.

In 2017, Li *et al.* [24] reported a significant depletion in PV output due to aerosols in China. Notably, in the Eastern Grid of China, the most significant impact on the direct irradiance could be observed, where it relatively dropped by 80%. The evidence from [24] highlighted that considering the high demand for electricity and severe air pollution in Western China, aerosols affected this area by reducing *POAI* up to 35%. In the evaluations of the impact of aerosols on tracking systems, with respect to the point that tracking systems mainly operate with direct irradiance, it was shown that aerosols decreased the electricity output of tracking PV systems more (both one and two axes tracking systems) more than when compared to fixed arrays systems. It was indicated that

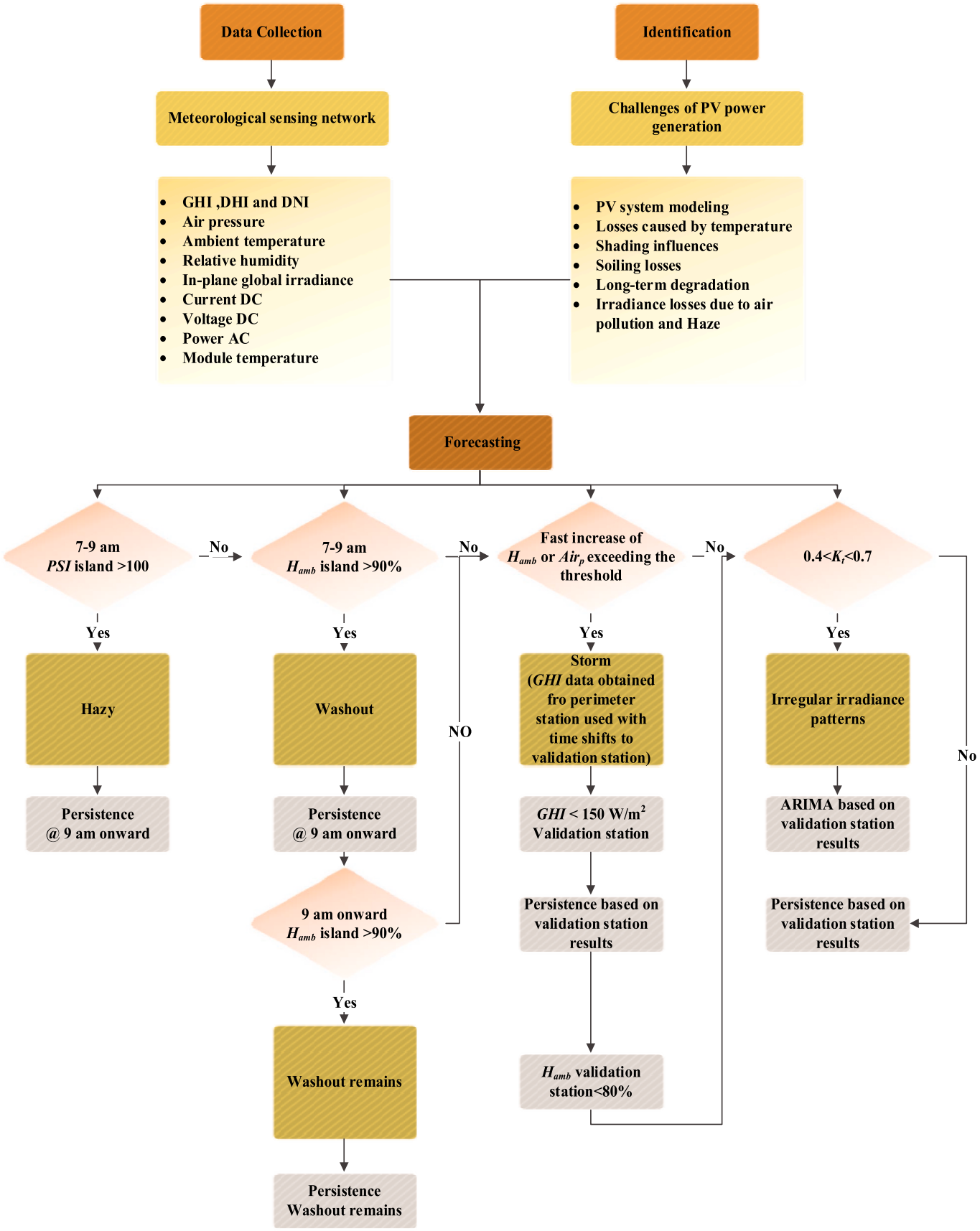

Fig. 9. Structure of Andre M. Nobre's methodology to forecast PV power generation in tropical climate zone (Figure reproduced from [89, 90]).

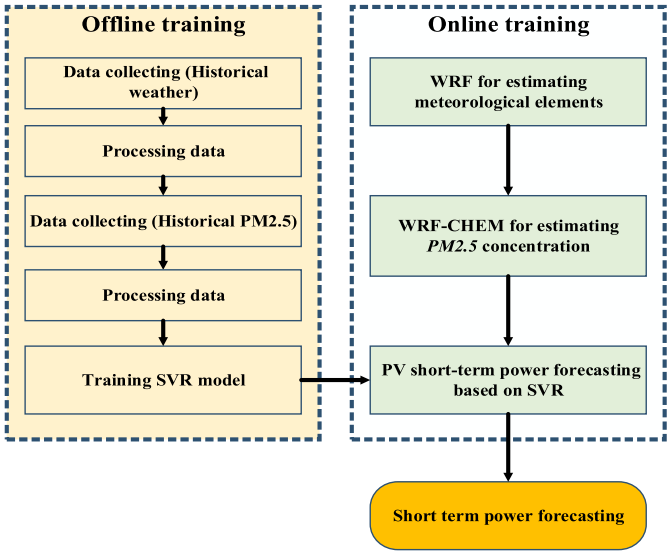

Fig. 10. Process of model training and power forecasting considering aerosols (reproduced from [74]).

there is an average 21% reduction of *POAI* for fixed systems and 34% for two axes over eastern China yearly. The vital role of clouds on surface radiation was also observed, where during the winter, the impact of aerosols on solar resources over the Northern Grid and the Eastern Grid of China is the same as clouds. They concluded that when considering the high potential of western China for solar energy generation, significant impacts of aerosols on direct *POAI* across this region should be considered.

In 2019, Sweerts *et al.* [110] concluded that air pollution resulted in an average reduction of 11–15% in PV power potential between 1960 and 2015 in the mainland of China. The link between observed surface radiation and sulfur dioxide and black carbon emissions points to air pollution control regulations and carbon footprints reduction strategies as essential tools to increase surface irradiance. Their surprising results imply that returning China's radiation levels to those of the 1960s could result in a 12–13% boost in PV energy generation in this country [110], corresponding to an additional 14 TWh of power generated with 2016 PV capacity and 51–74 TWh with expected 2030 PV capacity. As of 2016, China had more than 445 million households [181, 182] each person consumed almost 610 kWh [183](each household consumed almost 1900 kWh; therefore, that 14 TWh of PV losses caused by urban haze in 2016, could provide additional electricity of more than 7.3 million households in that year or almost 23 million people. Finally, upon reaching surface irradiance levels of 1960 could yield economic gains of US$1.9 billion in 2016 and US$4.6–6.7 billion in 2030. These results raise important questions about liability for polluters that are responsible for the economic losses resulting from pollution-caused haze on PV owners. This is an area important to policy makers for future work.

Del Hoyo *et al.* [27] in 2020 showed that haze decreased *GHI* and *DNI* by 3.5 % and 14.1% in Chile, respectively, while *DHI* increased by 35.4% simultaneously. Mono c-Si and a-Si PV technologies experienced a 7.2% and 8.7% reduction in their annual outputs. Finally, a noteworthy impact on PV modules due to aerosols has been reported in Chile [27], in which CPV power production was primarily affected by aerosols. i.e., a 16.4 % reduction in the annual output of this system was measured. This is in line with Li *et al.* [24] results because of more sensitivity of CPV systems to *DNI*, as previously reported that *DNI* decreased more than *GHI* and *DHI*, hence this outcome is evident. Son *et al.* at the same time [151] showed that *PM10* and *PM2.5* lead to a reduction in power generation by 14.2% - 14.9% for Yeongam installation and 9.8% - 16.1% for Eunpyeong installation in South Korea, respectively. Recent studies in China show severe effects of urban and anthropogenic haze on PV systems. Wu *et al.* [112] implied that the PV output of power plants in Hangzhou, decreased by 5.25 ± 1.19% and 6 ± 1.16% due to urban haze in 2017 and 2018, respectively. Furthermore, the effect of urban haze on PV power plants was more severe in Tianjin, where had experienced PV power reduction of 8.77 ± 0.9% for one year since Dec 2018.

3.2. Global haze

It is clear that the haze phenomenon is not limited to specific countries and is common worldwide. Shaddick *et al.* [184] reported that half of the world's population is experiencing increasing air pollution. Global haze as well [185] contributed to the growing trends in global warming, and these two are tied together. As PV performance also decreases with temperature, global warming, in general, reduces PV performance (although in snowy regions, it can decrease snow-related losses [186-191]). There are comprehensive studies in the literature covering the worldwide haze in their investigations of PV systems. Bergin *et al.* [55] in 2017 reported that PM affecting PV systems is primarily constituted of dust (92%), minor contributions from organic carbon (4%), ions (4%), and elemental carbon (0.01%). They proved that ambient and deposited PM on PV modules (i.e. soiling) have almost the same contributions in decreasing PV energy production [55].

In Fig. 11, there are important results discussed by Bergin *et al.* [55], which illustrates the effect of deposited and ambient PM on the trend in available energy for annual solar energy generation worldwide. Generally, both dusty and polluted regions have experienced noticeable effects, with significant declines in northern India, which is affected by both. Finally, their findings imply huge destructive impacts (irradiation degradation and soiling) of urban PM on PV performance, where a 17-25 % reduction in energy production has been reported across India (~1 GW loss) and China (~11 GW loss).

In 2018, Peters *et al.* [42] showed that Delhi, Beijing, and Singapore could experience a reduction of solar irradiance of 11.5 %, 9.1 %, and 2%, respectively. For other locations, Fig. 12 illustrates relative insolation losses, P_{PV} reductions, and *POAI* absolute values along with the losses in *POAI*. A method is needed whereby the economic losses for PV power generators would be compensated by prorating the liability of haze generators by their ratio of total emissions. Considerably more research is needed in this area, although there have been some attempts to quantify the economic losses PV generators suffer from haze in addition to those mentioned above. Peters *et al.* [42] estimations on revenue losses to PV power plants stack holders caused by urban haze in 2016, revealed about 0.78, 0.37, 2.4, 2.1, and 5.9-9.3 U.S. million dollars losses for Delhi (India), Kolkata (India), Beijing (China), Shanghai (China) and Los Angeles (US), respectively [42, 192, 193].

A recent study by Peters and Buonassisi [59] indicated that by the end of the century, the reduction in PV power performance considering different scenarios can range between 0.37 % and 2.5 % [0.37 % to 1.25 % for CdTe and 0.7 to 2.5 % for c-Si] due to the presence of water and aerosols in the atmosphere and global temperature rise. A specific objective for PV installations is to continue to focus on more efficient solar cell technologies and the development of solar energy infrastructure. In Fig. 13a by Peters and Buonassisi [59], a consistently more significant drop in insolation of east of 100 °E is seen, with insolation reduces by almost 0.8 W/m^2 per year compared to the remaining regions. Additionally, an average global warming rate of 0.02 K per year was derived. As demonstrated in Fig. 13b, an upsurge in *TPW* is observed, which results in the reduction of T_{TPW} throughout the majority of the Northern and Southern hemispheres. On the other hand, the examination of T_{AOD} points to more transmission in most of the earth. It was, however, noted that transmission changes due to aerosols are the most difficult to quantify. As a final point displayed in Fig. 13c, yields increased in South America and Africa and some regions of Europe but decreased in Northern Africa and America, whereas *PR* for the investigated Si PV technology decreased by an average of 0.04 % annually from

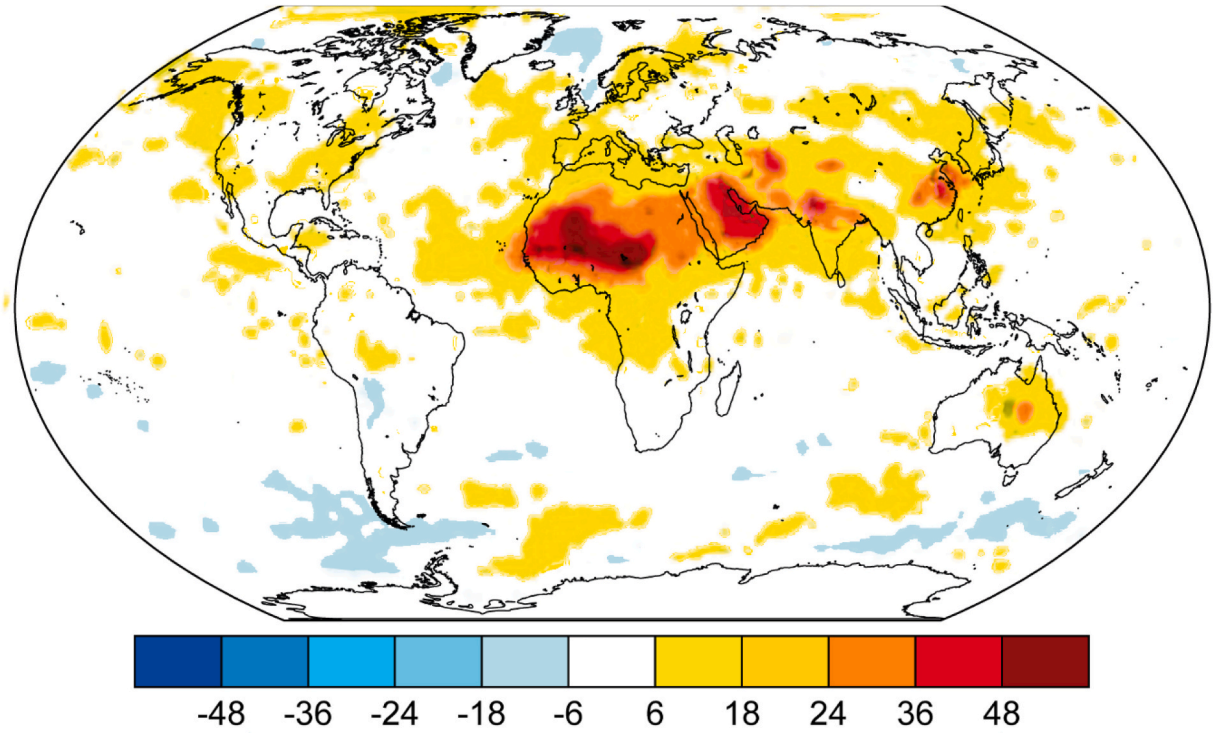

Fig. 11. Annual reduced visible solar energy as a result of ambient and accumulated particulate matter (figure from [55] ,[31] samples collected during February and March 2016 in Ahmadabad, India)

2006 to 2015.

Table 4 summarises a wide range of publications from all over the world collaborating to understand the impact of haze on PV performance by comparing year of publication, their location of study, time span of analysis and experiments, the used solar technology and module settings, haze concentration within the period of analysis, haze degradation indicator such as P_{out}, *CF*, or *POAI*, and reduction rate in the parameters along with reasons for the degradation.

4. Solutions to haze

There are well-known solutions in the literature to overcome haze and its associated consequences on PV power plants, including mitigating air pollution levels by employing renewable energy sources [24, 112] and preventing and controlling dust storms [28, 40, 195-199] and bushfires [26, 40, 46, 105, 200-203]. Since haze is mainly caused by emissions, defining policy measures and plans to reach net-zero carbon will have a positive impact not only on increased temperature losses on PV but also on haze-related PV losses. Furthermore, it is clear that national and local strategies and policies in each country to reduce carbon and PM emissions would positively impact PV performance. For example, polluted cities such as Delhi and Beijing are more affected by the haze. Numerous policymakers are now taking action to address air pollution concerns in these cities. As many cities across the world have proven that committed policies and the utilization of renewable energy systems can enhance air quality. Vitoria-Gasteiz in Spain, Montreal in Canada, Lisbon in Portugal, Medellin in Colombia, and Seoul in South Korea are notable examples of cities that have reduced air pollution from 28% to 63% [204]. China has established an effective plan against anthropogenic haze, which appears to be working in areas such as Beijing and Tianjin [42, 205, 206]. In places where anthropogenic haze is a significant issue, emissions restrictions would also be required to boost solar energy generation. Similar to concerns of carbon emissions liability [207-214], as PV power generation becomes more ubiquitous, there are unanswered questions about the liability of haze generators for reduction in output of both PV systems (as well as the reductions in agricultural output in India [215, 216], the U.S. [217, 218], and China [219, 220]). Decision-makers should implement pollution controls in light of the enormous potential benefits to public health, air quality and solar energy generation [55]. For example, by replacing all coal-fired power plants with PV in the U.S. generating an equivalent amount of electricity, over 52,000 premature deaths per year would be prevented [221]. Globally, high levels of political efforts have been made such as 2015 United Nations climate change conference (COP 21) [222] and COP 26 [223]. Serious actions to reach these conferences' goals, however, must be taken.

Other important solutions are to deploy more efficiencient technologies for areas frequently experiencing haze or develop and use new solar energy technologies with higher efficiencies. As discussed in this paper, higher band-gap PV technologies are more vulnerable to haze. This outcome could lead to PV manufacturers designing PV modules that perform better (efficiency-wise) in the regions that experience frequent haze, as proposed by Zhang *et al.* [49]. Moreover, in terms of electricity grid reliability, and because scattering and extinction of light caused by air pollution reduce the available solar resource, current solar-powered applications operating under haze conditions have reliability concerns that are an obstacle to distributed solar energy power grid [42, 224, 225]. Hence, a more reliable electricity grid can be had by increasing the efficiency of solar cells and reducing PV systems' vulnerability to haze [59].

The accumulation of haze particles on PV modules (considered soiling) is a considerable effect that should not be neglected. A study by Bergin *et al.* [55] proves that increasing the time for solar panels cleaning could reduce the output of these systems considerably, highlighting the significance of solar PV system cleaning in areas with high levels of dust and anthropogenic PM. As a result, a cleaning schedule should be a point of attention for solar power plants in some regions to reduce losses. Different cleaning methodologies have been presented in the literature [226-231] and employing new efficient technologies for dust removal and cleaning can be convenient way to overcome problems

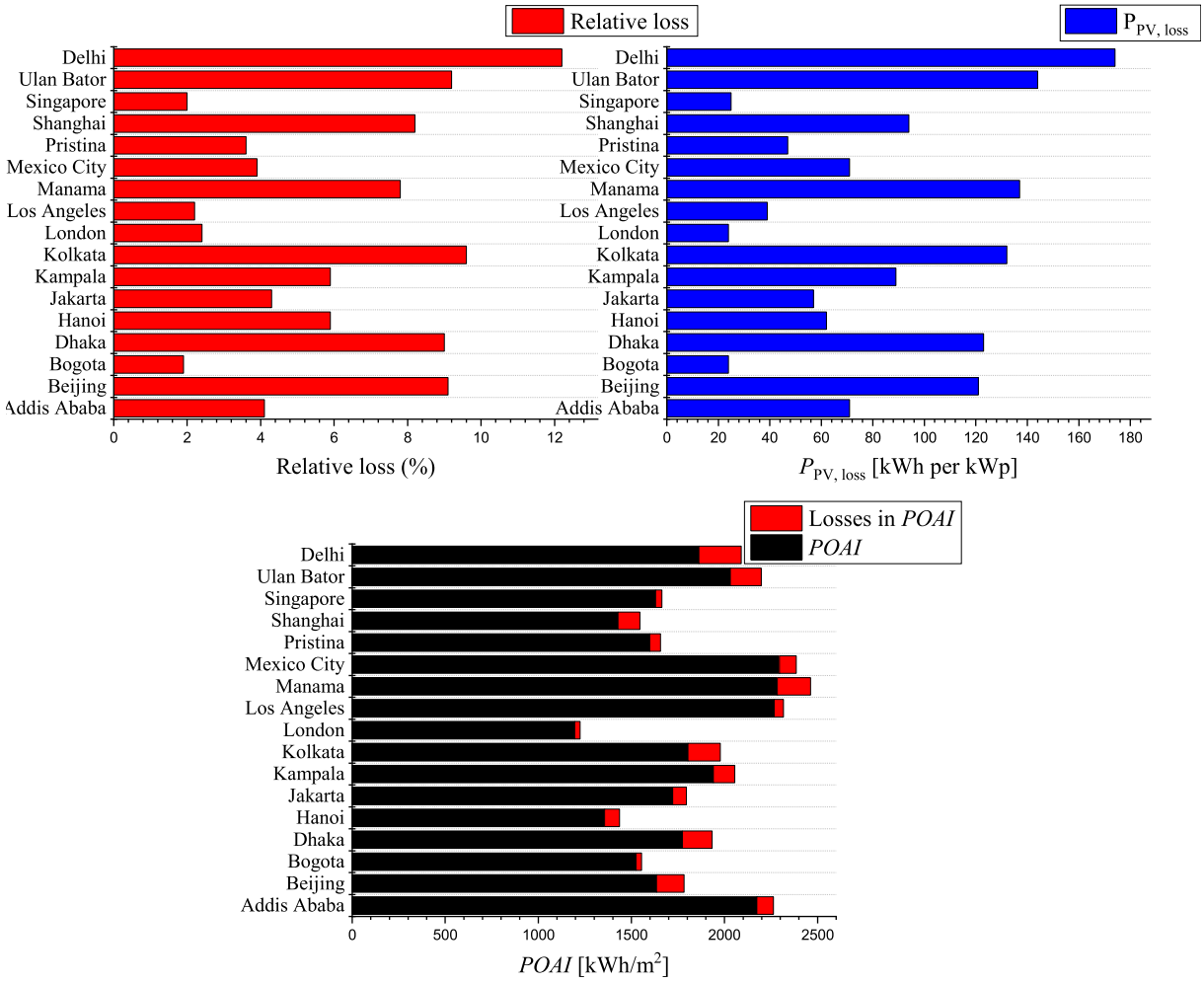

Fig. 12. Relative insolation losses for 16 cities, $P_{PV,\ loss}$ and *POAI* with absolute loss in *POAI* (data from [42]).

associated with soiling, such as electrostatic dust removal system (EDS) [232, 233], robotic cleaning [234], or anti-soiling coatings such as super hydrophobic [235] and super hydrophilic materials [236].

5. Future studies

Researchers have made great efforts to quantify the impact of haze on PV energy generation, there are still numerous research gaps in this context, which are crucial to be addressed in the future to help accelerate a sustainable future. According to the comprehensive literature review performed here, the following insghts can be suggested in future studies:

1. Sizing of PV power plants for different climate zones should consider haze and air pollution in the future, as different PV technologies sre affected differently by haze. For example, for low pollution regions, higher bandgap solar cells may be the optimal choice.
2. New clear sky models such as [128] can be used for investigating the effect of haze on PV modules and their results can be compared to previously used models [27, 77, 79].
3. Controlled indoor experiments in laboratory conditions can be conducted to correlate PV output and haze density (particulate matter and aerosol concentration) by defining relationships between PV output and haze concentration by investigating I-V characteristics.
4. Both short-term and long-term forecasting of haze implications on PV modules can be developed based on AI methodologies to prepare applicable tools and strategies for solar energy investors. For instance, advanced ANN such as MLP [161] methods can be developed for accurate forecasting of PV power plants experiencing severe haze.
5. For future studies, impact of haze on spectral albedo [237-240] and its consequences on PV output should be investigated in more refined researches.
6. Forecasting the impact of haze on the other solar energy technologies such as LCPV-HCPV [117, 118, 147, 148, 173-177] should be discussed in the future.
7. The role of different weather conditions such as rainy, cloudy weather and snowy weather conditions on the impacts of haze on PV generation has not been investigated yet. In furture studies, correlation between various weather conditions and haze can be considered to obtain a more complete understanding of the impact of haze on PV power generation.
8. Developing energy policy is needed that provides useful strategies to minimize haze and air pollution in communities, such as China Air Oollution Plan [42, 205, 206], which reduces haze effects on the PV industry. For example, future research studying the effects of haze on PV modules should cover financial analysis based on the levelized cost of electricity to quantify the liability for haze-generating

[3] Direct link: https://pubs.acs.org/doi/10.1021, Further permissions related to the material excerpted should be directed to the ACS.

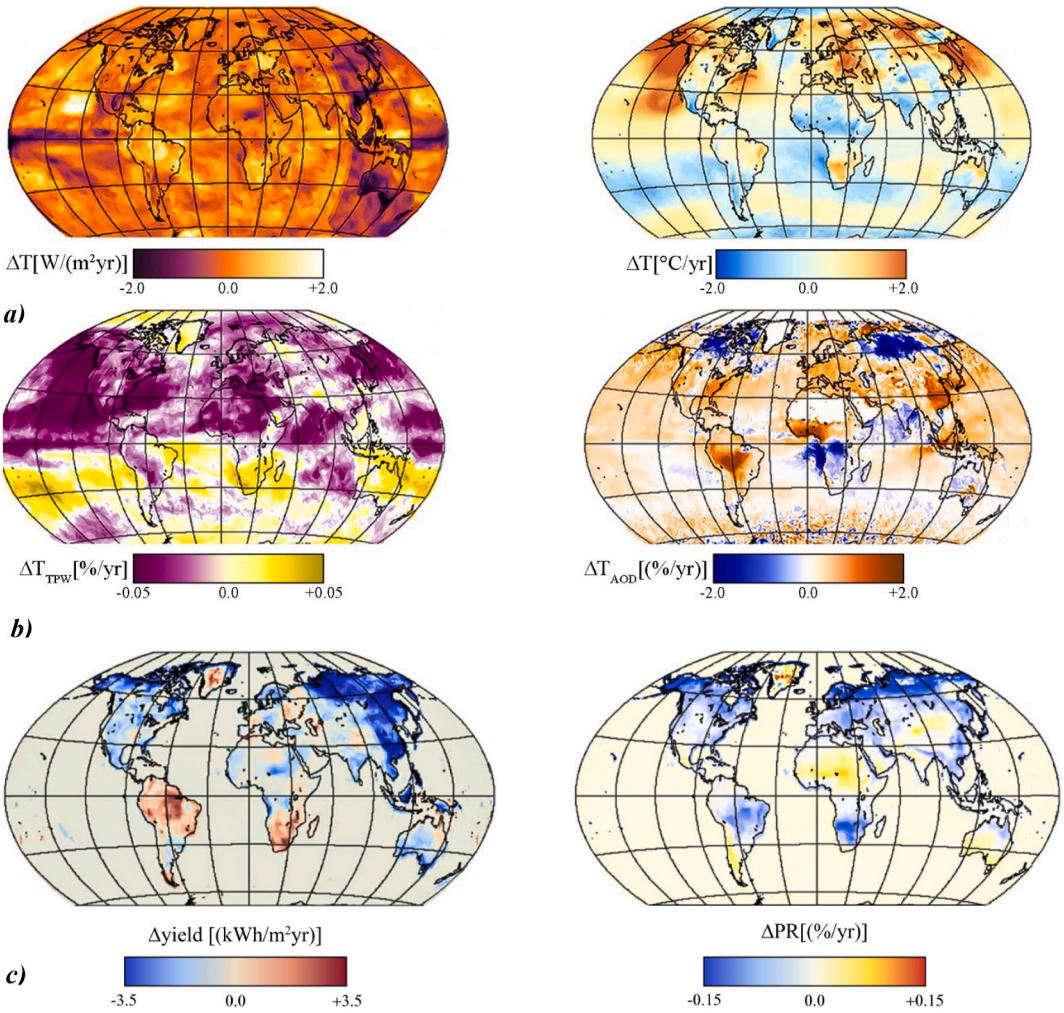

Fig. 13. Changes in PV power generation related parameters within the time span of 2006 to 2015. a) Changes in insolation and temperature b) direct TPW and AOD light transmission, and c) Y and PR (figures from [59]).

pollutors to promote sustainable development of renewable enegy across the world.

9. More research is required for regions lacking information of the effects of local haze and PV. Most of the research articles are limited to eastern Asia and China. Developing and reproducing these studies in other countries are required, particularly in the global south. For example, Australia, one of the pioneer countries in solar energy penetration [241], has recently suffered from bushfires and haze induced by these bushfires, while research on the impacts of PV there are lacking. One limitation to the deployment of such studies is the high cost of scientific equipment. In addition, to the satellite based approaches discussed above it is also possible to reduce the costs of experimental equipment with low open source cost climate stations [242] that helps improve the accessibility to underfunded scientists.

6. Conclusion and recommendation

This review paper conducted a thorough investigation on different methodologies that examine the effects of haze on PV energy generation, distinguished the critical results, and identified the research gaps. A variety of methods based on data analysis and experiments have been employed in the literature to examine potential changes in irradiance, spectrum and the output of PV technologies due to haze. Robust tools such as pvlib and GSEE can be employed for investigating the potential effects of haze on PV energy generation. It has been shown that aerosols, PM, and haze can considerably reduce PV systems' output. Core findings in the literature can be reported as follows:

1) Reduction in irradiance is the most dominant contribution of haze, followed by spectrum changes and soiling of PM in haze events.
2) Generally, attenuation caused by haze in solar energy resources has been reported in the literature based on real-world data collection (up to 80% due to urban haze and 40% because of bushfire smoke).
3) Due to spectrum changes, higher bandgap PV technologies are by 20-40% more affected by the presence of haze and aerosols in the atmosphere than low bandgap semiconductors. Therefore, designing and establishing power plants in regions that experience haze periods frequently would be more complicated, and more factors such as the spectral impacts should be considered.
4) Substantial annual revenue loss to PV installers for different cities around the world in the scale of US million dollars have been found based on electricity value and local haze values. Although questions remain about the liability or polluters that results in haze-related PV losses.
5) *DNI* is more heavily affected by haze. Therefore tracking and concentrated solar energy systems would be more affected by the haze than fixed tilt angle systems.

Declaration of competing interest

The authors declare that they have no known competing financial interests or personal relationships that could have appeared to influence

Table.4
Summary of reports on the impact of haze on PV energy generation.

Year	Location	Duration of Analysis	PV Technology	Module Setting	PM Concentration range *(PM10, PM2.5, PSI, AQI, or API)*	Target Parameter (s)	Rate of Reduction by haze [%]	Reason of Reduction	Ref.
2001	Iran	10 months	Mono c-Si, Multi c-Si, Thin film	Different tilt angles	Not reported	P_{out} [W]	Up to 60 %	Urban haze and Pollution	[104]
2014	Singapore	1 month	a-Si c-Si	Optimum angle	Avg. *PSI* ≈*50-200*	*PR* [%]	Up to 7 % for a-Si, ≈ 0 % for c-Si	Bushfire smoke	[26]
2014	Singapore	1 month	Single-j a-Si, CdTe, CIGS, Double-j micromorph Si	Optimum angle	Avg. *PSI* ≈*50-200*	*EIR*	≈ 2% for a-Si, ≈ 2% for CdTe, ≈ 0% for CIGS, Slight increase for micromorph Si	Bushfire smoke	[46]
2015	Malaysia	1 month	Mono c-Si	Tracking PV, Fixed PV	Max *API=231* Min *API=65* Avg. *API=143*	P_{out} [W]	30 % for fixed Mono c-Si, 25 % for tracking Mono c-Si	Fire smoke	[103]
2016	Singapore	1 month	c-Si wafer-based	Optimum angle	Avg. *PSI* ≈ *50-200*	P_{out} [W]	Up to 25 %	Bushfire smoke	[89]
2016	Singapore	18 days	Mono c-Si Multi c-Si Mono hetero-j Single-j a-Si Triple-j a-Si Micro c-Si thin-film	Optimum angle, Different tilt angles	Avg. *PSI* ≈ *50-200*	*Y* [kWh/kWp]	≈ 15 % mono c-Si, Up to 18.4 % multi c-Si, ≈ 18.7 % multi c-Si Het, Up to 21.4 % single-j, Up to 24.7 % triple-j, ≈ 25.3 % micro c-Si thin film	Bushfire smoke	[79]
2016	China	1 year	PV (not reported)	Optimum angle	*PM2.5* (0- 35) μg/m^3 *PM2.5* (35 -75) μg/m^3 *PM2.5* (75-115) μg/m^3 *PM2.5*(115-250) μg/m^3	P_{out} [W]	≈ 0 ref ≈ 6.5 % ≈ 7.1 % ≈ 30 %	Urban haze	[194]
2017	Worldwide	1-3 months	Thin film CIS, Multi c-Si	Horizontal fixed	-	Available energy for solar generation [GW]	17-25 %	Urban haze	[55]
2017	Malaysia	1 months	Mono c-Si	Optimum angle	Max *PM 10*=275.2 μg/m^3 Min *PM 10*=23.2 μg/m^3 Avg. *PM 10*=105.6 μg/m^3	P_{out} [W]	17.8 %	Bushfire smoke	[105]
2017	China	12 years	PV, CSP	Optimum angle fixed, One axis tracking, Two axes tracking	Not reported	*POAI* [kWh/m^2/day]	Up to 80 % for direct *POAI* 25-35 % for average *POAI*	Urban haze	[24]
2018	Different locations	19 months	Si-PV GaAs CdTe Perovskite	Optimum angle fixed	*PM2.5* (50- 400) μg/m^3	Absorbed photon flux [1/m^2.s]	3.9-12.2 % Si-PV, 4.8-15.0 % GaAs, 5.2-16.1 % CdTe, 5.5-17.2 % Perovskite	Urban haze	[42]
2018	India	18 months	Si PV	Optimum angle	For every *PM2.5* 100 μg/m^3 Over 18 months	Q_{Annual} [kWh/m^2/day]	12±3% 11.5%	Urban haze	[178]
2019	China	55 years	PV (not reported)	Horizontal fixed, Optimum angle fixed, Horizontal tracking,	Not reported	*CF* [%]	11–15 %	Urban haze	[110]
2020	Chile	2 years	Mono c-Si a-Si CPV	Optimum angle for PV	Not reported	P_{out}, P_{PV}, P_{CPV} [W]	7.2 % mono c-Si annually, 8.7 % a-Si annually, 16.4 % CPV annually,	Urban haze	[27]
2020	China	2 years	PV (not reported)	Optimum angle	*PM2.5* (25- 41) μg/m^3 *PM2.5* (71- 109) μg/m^3 *PM2.5* (125- 183)μg/m^3	P_{PV} [W]	≈ 0 ref ≈ 6.14 % ≈ 19.57 % ≈ 46.1 %	Urban haze	[112]

(*continued on next page*)

Table.4 (*continued*)

Year	Location	Duration of Analysis	PV Technology	Module Setting	PM Concentration range *(PM10, PM2.5, PSI, AQI, or API)*	Target Parameter (s)	Rate of Reduction by haze [%]	Reason of Reduction	Ref.
					PM2.5 (156- 218) μg/m^3 Total		5.25-8.77% annually		
2020	Republic of Korea	3 years	PV (not reported)	Optimum angle	*PM2.5* of 15 μg/m^3 and *PM10* of 30 μg/m^3	P_{out} [W]	9.8-16.1 %	Urban haze	[151]
					PM2.5 of 75 μg/m^3 and *PM10* 150 μg/m^3		15.6-23.7 %		
2020	China	4 years	PV (not reported), CPV	Optimum angle Fixed for PV	Avg. *PM 2.5*= 50.8-99.5 μg/m^3	*G* [kWh/m^2/day]	7 to 21.8 % annually	Urban haze	[71]
2020	Italy	19 months	PV (not reported)	Optimum angle	*PM 2.5* mainly up to 50 μg/m^3	Q_{Annual} [kWh/m^2/day]	5 % annually	Urban haze	[157]
2021	USA	15 months	PV (not reported)	Optimum angle	*PM2.5* (50- 200) μg/m^3	P_{out},P_{PV} [W]	9.4-37.8 %	Bushfire smoke	[83]
2021	China	3 months	PV (not reported)	Optimum angle	*PM 2.5*= 73 μg/m^3 *PM 2.5*= 105 μg/m^3 Avg. *PM 2.5*= 35-75 μg/m^3	P_{out} [W]	39.7 % 49.6 % Totally 8.1 %	Urban haze	[106]
2021	Worldwide	10 years, 100 years	c-Si, CdTe	Not discussed	Not reported	*PR* [%]	From 2006-2015 (10 years):0.4 % By end of century (2100): 0.7-2.5 % c-Si, 0.38- 1.25 % CdTe	Haze, atmospheric water and global warming	[59]

the work reported in this paper.

Data availability

Data will be made available on request.

Acknowledgments

The Australian Government has partly supported this work through the Australian Renewable Energy Agency (ARENA) via a grant from the Australian Centre of Advanced Photovoltaics (ACAP). This work was partially supported by the Thompson Endowment and the Natural Sciences and Engineering Research Council of Canada.

Appendix A. Supplementary data

Supplementary data to this article can be found online at https://doi.org/10.1016/j.rser.2022.112796.

References

[1] IRENA. Renewable Energy Statistics ", https://public.tableau.com/views/IRENARETimeSeries/Charts?:embed=y&:showVizHome=no&publish=yes&:toolbar=no. [Accessed September 2021].
[2] Creutzig Felix, Peter Agoston, Christoph Goldschmidt Jan, Luderer Gunnar, Nemet Gregory, Pietzcker Robert C. The underestimated potential of solar energy to mitigate climate change. Nature Energy 2017;2(9):1–9.
[3] Haegel Nancy M, et al. Terawatt-scale photovoltaics: Trajectories and challenges. Science 2017;356(6334):141–3.
[4] IRENA. Country Rankings for PV solar energy (accessed September 2021), https://www.irena.org/Statistics/View-Data-by-Topic/Capacity-and-Generation/Country-Rankings.
[5] Branker Kadra, Pathak MJM, Pearce Joshua M. A review of solar photovoltaic levelized cost of electricity. Renewable and sustainable energy reviews 2011;15(9):4470–82.
[6] Wiser Ryan H, Bolinger Mark, Seel Joachim. Benchmarking utility-scale PV operational expenses and project lifetimes: results from a survey of US solar industry professionals. Berkeley, CA (United States): Lawrence Berkeley National Lab.(LBNL); 2020.
[7] Schmalensee Richard. The future of solar energy: an interdisciplinary MIT study. Energy Initiative, Massachusetts Institute of Technology; 2015.
[8] Atkin Peter, Farid Mohammed M. Improving the efficiency of photovoltaic cells using PCM infused graphite and aluminium fins. Solar Energy 2015/04/01/2015;114:217–28. https://doi.org/10.1016/j.solener.2015.01.037.
[9] Feldman David, Jones-Albertus Rebecca, Margolis Robert. Quantifying the impact of R&D on PV project financing costs. Energy Policy 2020;142:111525.
[10] Tan Zhongfu, Tan Qingkun, Rong Menglei. Analysis on the financing status of PV industry in China and the ways of improvement. Renewable and Sustainable Energy Reviews 2018;93:409–20.
[11] Feldman David J, Schwabe Paul D. Terms, Trends, and Insights on PV Project Finance in the United States. Golden, CO (United States): National Renewable Energy Lab.(NREL); 2018. 2018.
[12] Ghazi Sanaz, Ip Kenneth. The effect of weather conditions on the efficiency of PV panels in the southeast of UK. Renewable energy 2014;69:50–9.
[13] Liu Xiaoyong, et al. Chemical Characteristics and Potential Sources of PM2. 5 in Shahe City during Severe Haze Pollution Episodes in the Winter. Aerosol and Air Quality Research 2020;20.
[14] Kazem Ali A, Chaichan Miqdam T, Kazem Hussein A. Dust effect on photovoltaic utilization in Iraq: Review article. Renewable and Sustainable Energy Reviews 2014/09/01/2014;37:734–49. https://doi.org/10.1016/j.rser.2014.05.073.
[15] Vardoulakis Sotiris, Marks Guy, Abramson Michael J. Lessons learned from the Australian bushfires: climate change, air pollution, and public health. JAMA internal medicine 2020;180(5):635–6.
[16] CBC News. A look back at the 2021 B.C. wildfire season (accessed March, 2022), https://www.cbc.ca/news/canada/british-columbia/bc-wildfires-2021-timeline-1.6197751.
[17] Liu Shao-Kun, Cai Shan, Chen Yan, Xiao Bing, Chen Ping, Xiang Xu-Dong. The effect of pollutional haze on pulmonary functioneng, editor. J Thorac Dis 2016;8(1):E41–56. https://doi.org/10.3978/j.issn.2072-1439.2016.01.18.
[18] Ma Q, Liu Y, Liu C, Ma J, He H. A case study of Asian dust storm particles: chemical composition, reactivity to SO2 and hygroscopic properties," (in eng). J Environ Sci (China) 2012;24(1):62–71. https://doi.org/10.1016/s1001-0742(11)60729-8.
[19] Clinton Nicholas E, Gong Peng, Scott Klaus. Quantification of pollutants emitted from very large wildland fires in Southern California, USA. Atmospheric Environment 2006/06/01/2006;40(20):3686–95. https://doi.org/10.1016/j.atmosenv.2006.02.016.
[20] Clare Averill (Raytheon ITSS/JPL). The Size of Dust and Smoke. accessed Sep., 2021), https://earthobservatory.nasa.gov/images/5730/the-size-of-dust-and-smoke.
[21] Park Minhan, et al. Differential toxicities of fine particulate matters from various sources. Scientific Reports 2018/11/19 2018;8(1):17007. https://doi.org/10.1038/s41598-018-35398-0.
[22] Goudie Andrew S. Desert dust and human health disorders. Environment International 2014/02/01/2014;63:101–13. https://doi.org/10.1016/j.envint.2013.10.011.
[23] Johnston Fay H, et al. Unprecedented health costs of smoke-related PM2.5 from the 2019–20 Australian megafires. Nature Sustainability 2021/01/01 2021;4(1):42–7. https://doi.org/10.1038/s41893-020-00610-5.
[24] Li Xiaoyuan, Wagner Fabian, Peng Wei, Yang Junnan, Mauzerall Denise L. Reduction of solar photovoltaic resources due to air pollution in China. Proceedings of the National Academy of Sciences 2017;114(45):11867–72.
[25] Rayleigh Lord, XXXIV. On the transmission of light through an atmosphere containing small particles in suspension, and on the origin of the blue of the sky. The London, Edinburgh, and Dublin Philosophical Magazine and Journal of

Science 1899/04/01 1899;47(287):375–84. https://doi.org/10.1080/14786449908621276.
[26] Liu H, et al. The Impact of Haze on Performance Ratio and Short-Circuit Current of PV Systems in Singapore. IEEE Journal of Photovoltaics 2014;4(6):1585–92. https://doi.org/10.1109/JPHOTOV.2014.2346429.
[27] Del Hoyo Mirko, Rondanelli Roberto, Rodrigo Escobar. Significant decrease of photovoltaic power production by aerosols. The case of Santiago de Chile. Renewable Energy 2020;148:1137–49.
[28] Kazem Ali A, Chaichan Miqdam T, Kazem Hussein A. Dust effect on photovoltaic utilization in Iraq. Renewable and Sustainable energy reviews 2014;37:734–49.
[29] Saidan Motasem, Ghani Albaali Abdul, Alasis Emil, Kaldellis John K. Experimental study on the effect of dust deposition on solar photovoltaic panels in desert environment. Renewable Energy 2016;92:499–505.
[30] Jones ADLA, Roberts DL, Slingo A. A climate model study of indirect radiative forcing by anthropogenic sulphate aerosols. Nature 1994;370(6489):450–3.
[31] Schwartz Stephen E. The whitehouse effect—Shortwave radiative forcing of climate by anthropogenic aerosols: An overview. Journal of Aerosol Science 1996;27(3):359–82.
[32] Hansen J, Sato Mki, Ruedy R. Radiative forcing and climate response. Journal of Geophysical Research: Atmospheres 1997;102(D6):6831–64.
[33] Xia X, Li Z, Wang P, Chen H, Cribb M. Estimation of aerosol effects on surface irradiance based on measurements and radiative transfer model simulations in northern China. Journal of Geophysical Research: Atmospheres 2007;112(D22).
[34] Devi Kanniah Kasturi, Beringer Jason, Tapper Nigel J, Long Chuck N. Aerosols and their influence on radiation partitioning and savanna productivity in northern Australia. Theoretical and Applied Climatology 2010;100(3):423–38.
[35] Foyo-Moreno I, Alados I, Antón M, Fernández-Gálvez J, Cazorla A, Alados-Arboledas L. Estimating aerosol characteristics from solar irradiance measurements at an urban location in southeastern Spain. Journal of Geophysical Research: Atmospheres 2014;119(4):1845–59.
[36] Younis A, Alhorr Y. Modeling of dust soiling effects on solar photovoltaic performance: A review. Solar Energy 2021/05/15/2021;220:1074–88. https://doi.org/10.1016/j.solener.2021.04.011.
[37] Weiping Zhao, Yukun Lv, Zian Wei, Weiping Yan, and Qingwen Zhou, "Review on dust deposition and cleaning methods for solar PV modules," Journal of Renewable and Sustainable Energy, vol. 13, no. 3, p. 032701, 2021/05/01 2021, doi: 10.1063/5.0053866.
[38] Shaju Anitha, Chacko Rani. Soiling of photovoltaic modules- Review. IOP Conference Series: Materials Science and Engineering 2018/08/29 2018;396:012050. https://doi.org/10.1088/1757-899x/396/1/012050.
[39] Klemens Ilse, et al. Techno-Economic Assessment of Soiling Losses and Mitigation Strategies for Solar Power Generation. Joule 2019;3(10):2303–21. https://doi.org/10.1016/j.joule.2019.08.019. /10/16/2019.
[40] Maghami Mohammad Reza, Hizam Hashim, Gomes Chandima, Radzi Mohd Amran, Rezadad Mohammad Ismael, Hajighorbani Shahrooz. Power loss due to soiling on solar panel: A review. Renewable and Sustainable Energy Reviews 2016/06/01/2016;59:1307–16. https://doi.org/10.1016/j.rser.2016.01.044.
[41] Figgis B, Ennaoui A, Ahzi S, Rémond Y. Review of PV soiling measurement methods. International Renewable and Sustainable Energy Conference (IRSEC), 14-17 Nov. 2016. p. 176–80. https://doi.org/10.1109/IRSEC.2016.7984027. 2016 2016.
[42] Peters IM, Karthik S, Liu H, Buonassisi T, Nobre A. Urban haze and photovoltaics. Energy & Environmental Science 2018;11(10):3043–54.
[43] Field Halden. Solar cell spectral response measurement errors related to spectral band width and chopped light waveform. In: Conference Record of the Twenty Sixth IEEE Photovoltaic Specialists Conference-1997. IEEE; 1997. p. 471–4.
[44] Heydenreich Wolfgang, Müller Björn, Reise Christian. Describing the world with three parameters: a new approach to PV module power modelling. In: European Photovoltaic Solar Energy Conference; 2008. p. 1–5. ," in 23rd.
[45] Reich Nils H, Mueller Bjoern, , Alfons Armbruster, Wilfried GJHM Van Sark, Kiefer Klaus, Reise Christian. Performance ratio revisited: is PR> 90% realistic? Progress in Photovoltaics: Research and Applications 2012;20(6):717–26.
[46] Ye Jia Ying, Reindl Thomas, Aberle Armin G, Walsh Timothy M. Effect of solar spectrum on the performance of various thin-film PV module technologies in tropical Singapore. IEEE Journal of Photovoltaics 2014;4(5):1268–74.
[47] Nann S, Emery K. Spectral effects on PV-device rating. Solar Energy Materials and Solar Cells 1992/08/01/1992;27(3):189–216. https://doi.org/10.1016/0927-0248(92)90083-2.
[48] Ahsan Syed M, Khan Hassan A. Performance comparison of CdTe thin film modules with c-Si modules under low irradiance. IET Renewable Power Generation 2019;13(11):1920–6.
[49] Zhang Chenlong, Gwamuri Jephias, Andrews Rob, Pearce Joshua M. Design of multijunction photovoltaic cells optimized for varied atmospheric conditions. International Journal of Photoenergy 2014:2014.
[50] V Salinas Santo, et al. Physical and optical characteristics of the October 2010 haze event over Singapore: A photometric and lidar analysis. Atmospheric Research 2013;122:555–70.
[51] Behrendt Tanja, Jan Kuehnert, Hammer Annette, Lorenz Elke, Betcke Jethro, Heinemann Detlev. Solar spectral irradiance derived from satellite data: A tool to improve thin film PV performance estimations? Solar Energy 2013;98:100–10.
[52] Jacobson Mark Z. Isolating nitrated and aromatic aerosols and nitrated aromatic gases as sources of ultraviolet light absorption. Journal of Geophysical Research: Atmospheres 1999;104(D3):3527–42.
[53] Martins VS, Lyapustin A, de Carvalho LAS, Barbosa CCF, Novo EMLM. Validation of high-resolution MAIAC aerosol product over South America. Journal of Geophysical Research: Atmospheres 2017/07/27 2017;122(14):7537–59. https://doi.org/10.1002/2016JD026301.
[54] Holben Brent N, et al. AERONET—A federated instrument network and data archive for aerosol characterization. Remote sensing of environment 1998;66(1):1–16.
[55] H Bergin Mike, Ghoroi Chinmay, Dixit Deepa, Schauer James J, Shindell Drew T. Large reductions in solar energy production due to dust and particulate air pollution. Environmental Science & Technology Letters 2017;4(8):339–44.
[56] Gavin Schmidt Dr, GCM ModelE GISS. https://www.giss.nasa.gov/tools/modelE/. [Accessed December 2021]. accessed.
[57] NASA. NASA's Ozone Monitoring Instrument (OMI). accessed Dec., 2021), https://www.nasa.gov/mission_pages/aura/spacecraft/omi.html.
[58] NASA. NASA's Moderate Resolution Imaging Spectroradiometer (MODIS). accessed Dec., 2021), https://modis.gsfc.nasa.gov/.
[59] Marius Peters Ian, Buonassisi Tonio. How changes in worldwide operating conditions affect solar cell performance. Solar Energy 2021;220:671–9.
[60] NASA. "NASA's Clouds and the Earth's Radiant Energy System (CERES)." https://ceres.larc.nasa.gov/ (accessed Dec., 2021).
[61] Rienecker Michele M, et al. MERRA: NASA's Modern-Era Retrospective Analysis for Research and Applications," (in English). Journal of Climate 15 Jul. 2011 2011;24(14):3624–48. https://doi.org/10.1175/JCLI-D-11-00015.1.
[62] Pfenninger Stefan, Staffell Iain. Long-term patterns of European PV output using 30 years of validated hourly reanalysis and satellite data. Energy 2016/11/01/2016;114:1251–65. https://doi.org/10.1016/j.energy.2016.08.060.
[63] Molod A, Takacs L, Suarez M, Bacmeister J. Development of the GEOS-5 atmospheric general circulation model: evolution from MERRA to MERRA2. Geosci. Model Dev. 2015;8(5):1339–56. https://doi.org/10.5194/gmd-8-1339-2015.
[64] Müller Richard, Pfeifroth Uwe, Träger-Chatterjee Christine, Cremer Roswitha, Trentmann Jörg, Hollmann Rainer. Surface solar radiation data set-Heliosat (SARAH)," Climate Monitoring Satellite Application Facility. Germany: Darmstadt; 2015.
[65] AIRS Science Team/Joao Texeira. "AIRS/Aqua L3 Daily Standard Physical Retrieval (AIRS-only) 1 degree × 1 degree V006." Goddard Earth Sciences Data and Information Services Center (GES DISC),. (accessed.
[66] Schmidt Gavin A, et al. Configuration and assessment of the GISS ModelE2 contributions to the CMIP5 archive. Journal of Advances in Modeling Earth Systems 2014;6(1):141–84.
[67] Shindell Drew T, et al. Interactive ozone and methane chemistry in GISS-E2 historical and future climate simulations. Atmospheric Chemistry and Physics 2013;13(5):2653–89.
[68] Gueymard CA. SMARTS2: a simple model of the atmospheric radiative transfer of sunshine: algorithms and performance assessment. 1995 [Online]. Available: http://www.fsec.ucf.edu/en/publications/pdf/fsec-pf-270-95.pdf.
[69] Gueymard Christian, SMARTS2. a simple model of the atmospheric radiative transfer of sunshine: algorithms and performance assessment. FL: Florida Solar Energy Center Cocoa; 1995.
[70] Gueymard Christian A. Parameterized transmittance model for direct beam and circumsolar spectral irradiance. Solar Energy 2001;71(5):325–46.
[71] Zhang Liyuan, Zhang Yue, Yi Xiaoxiao, Yang Yiqi, Zhao Min, Zhou Jieting. Seasonal variations of the impact of urban aerosol pollution on distributed solar photovoltaic generation of nine megacities in China. Urban Climate 2020;34:100723.
[72] Pitchford Marc, Malm William, Schichtel Bret, Kumar Naresh, Douglas Lowenthal, Jenny Hand. Revised algorithm for estimating light extinction from IMPROVE particle speciation data. Journal of the Air & Waste Management Association 2007;57(11):1326–36.
[73] Malm William C, Sisler James F, Huffman Dale, Eldred Robert A, Cahill Thomas A. Spatial and seasonal trends in particle concentration and optical extinction in the United States. Journal of Geophysical Research: Atmospheres 1994;99(D1):1347–70.
[74] Liu Wenjie, et al. Short-term PV power prediction considering the influence of aerosol. In: IOP Conference Series: Earth and Environmental Science, 585; 2020, 012017. 1: IOP Publishing.
[75] Tie Xuexi, Geng Fuhai, Peng Li, Gao Wei, Zhao Chunsheng. Measurement and modeling of O3 variability in Shanghai, China: Application of the WRF-Chem model. Atmospheric Environment 2009;43(28):4289–302.
[76] DeNero Steven P. Development of a source oriented version of the WRF-Chem model and its application to the California Regional PM10/PM2. 5 air quality study. Davis: University of California; 2012.
[77] Reno Matthew J, Hansen Clifford W. Identification of periods of clear sky irradiance in time series of GHI measurements. Renewable Energy 2016/05/01/2016;90:520–31. https://doi.org/10.1016/j.renene.2015.12.031.
[78] Holmgren William F, Hansen Clifford W, Mikofski Mark A. pvlib python: A python package for modeling solar energy systems. Journal of Open Source Software 2018;3(29):884.
[79] Nobre André M, et al. On the impact of haze on the yield of photovoltaic systems in Singapore. Renewable Energy 2016;89:389–400.
[80] Yang Dazhi, Walsh Wilfred M, Jirutitijaroen Panida. Estimation and Applications of Clear Sky Global Horizontal Irradiance at the Equator. Journal of Solar Energy Engineering 2014;136(3). https://doi.org/10.1115/1.4027263.
[81] Zhou Zhigao, et al. Estimation of the losses in potential concentrated solar thermal power electricity production due to air pollution in China. Science of The Total Environment 2021;784:147214. https://doi.org/10.1016/j.scitotenv.2021.147214. /08/25/2021.

[82] Yang Kun, Koike Toshio, Ye Baisheng. Improving estimation of hourly, daily, and monthly solar radiation by importing global data sets. Agricultural and Forest Meteorology 2006;137(1-2):43–55.

[83] Gilletly SD, Jackson ND, Staid A. Quantifying Wildfire-Induced Impacts to Photovoltaic Energy Production in the western United States. IEEE 48th Photovoltaic Specialists Conference (PVSC), 20-25 June 2021 2021. 2021. p. 1619–25. https://doi.org/10.1109/PVSC43889.2021.9518514.

[84] Andrews Robert W, Stein Joshua S, Hansen Clifford, Riley Daniel. Introduction to the open source PV LIB for python Photovoltaic system modelling package. IEEE 40th photovoltaic specialist conference (PVSC). IEEE; 2014. p. 170–4. 2014.

[85] Joshua S Stein William F Holmgren, Forbess Jessica, Hansen Clifford W. PVLIB: Open source photovoltaic performance modeling functions for Matlab and Python. In: ieee 43rd photovoltaic specialists conference (pvsc). IEEE; 2016. p. 3425–30. 2016.

[86] Holmgren William, Andrews Robert, Lorenzo Antonio, Stein Joshua. PVLIB Python 2015:1–5. 2015.

[87] Gunda M Hopwood T, Mendoza H. A python package for PV operators & researchers-pvOps. accessed Dec., 2021), https://pypi.org/project/pvops/.

[88] Rojas Redlich García, Alvarado Natalia, Boland John, Rodrigo Escobar, Castillejo-Cuberos Armando. Diffuse fraction estimation using the BRL model and relationship of predictors under Chilean, Costa Rican and Australian climatic conditions. Renewable Energy 2019;136:1091–106.

[89] Nobre Andre M, et al. PV power conversion and short-term forecasting in a tropical, densely-built environment in Singapore. Renewable Energy 2016;94:496–509.

[90] Maia Nobre André. Short-term solar irradiance forecasting and photovoltaic systems performance in a tropical climate in Singapore. 2015.

[91] Kong Junhyuk, Oh Seongmun, Jung Jaesung, Lee Ineung. Improving the Accuracy of Photovoltaic Generation Forecasting by Considering Particulate Matter Variables. IEEE Power & Energy Society General Meeting (PESGM). IEEE; 2020. p. 1–5. 2020.

[92] Hanif Jufri Fauzan, Jung Jaesung. Photovoltaic generation forecasting using artificial neural networks model with input variables and model parameters selection algorithm in korea. International Journal of Machine Learning and Computing 2017;7(5):156–61.

[93] Zhao Zhen, et al. SVM based cloud classification model using total sky images for PV power forecasting. IEEE Power & Energy Society Innovative Smart Grid Technologies Conference (ISGT). IEEE; 2015. p. 1–5. 2015.

[94] Veronika Dorogush Anna, Ershov Vasily, Gulin Andrey. CatBoost: gradient boosting with categorical features support. arXiv preprint arXiv:1810.11363; 2018.

[95] Catboost. https://github.com/catboost/catboost. [Accessed December 2021]. accessed.

[96] Wang Yong. IH Witten Inducing Model Trees for Continuous Classes. In: Proc. of the 9th European Conf. on Machine Learning Poster Papers; 1997.

[97] Perez Richard, et al. Comparison of numerical weather prediction solar irradiance forecasts in the US, Canada and Europe. Solar Energy 2013/08/01/2013;94:305–26. https://doi.org/10.1016/j.solener.2013.05.005.

[98] Lan Feng, Qin Wenmin, Wang Lunche, Lin Aiwen, Zhang Ming. Comparison of artificial intelligence and physical models for forecasting photosynthetically-active radiation. Remote Sensing 2018;10(11):1855.

[99] Friedman Jerome H. Multivariate adaptive regression splines. The annals of statistics 1991:1–67.

[100] Cleveland William S, Grosse Eric, Shyu William M. Local regression models. In: Statistical models in S. Routledge; 2017. p. 309–76.

[101] Belsley David A, Edwin Kuh, Welsch Roy E. Regression diagnostics: Identifying influential data and sources of collinearity. John Wiley & Sons; 2005.

[102] Pearson Karl. VII. Note on regression and inheritance in the case of two parents. proceedings of the royal society of London 1895;58(347-352):240–2.

[103] Maghami Mohammadreza, Hizam Hashim, Gomes Chandima, Hajighorbani Shahrooz, Rezaei Nima. Evaluation of the 2013 southeast asian haze on solar generation performance. PloS one 2015;10(8):e0135118.

[104] Asl-Soleimani E, Farhangi Sh, Zabihi MS. The effect of tilt angle, air pollution on performance of photovoltaic systems in Tehran. Renewable Energy 2001;24(3-4):459–68.

[105] Rahim Nasrudin Abd, Mohammed Mohd Fayzul, Eid Bilal M. Assessment of effect of haze on photovoltaic systems in Malaysia due to open burning in Sumatra. IET Renewable Power Generation 2017;11(3):299–304.

[106] Chen Wei, et al. The impact of haze on photovoltaic systems: a case study. Energy Sources, Part A: Recovery, Utilization, and Environmental Effects 2021:1–17.

[107] National Laboratories Sandia. Sandia PV Array Performance Model (SAPM) (accessed Feb., 2022), https://pvpmc.sandia.gov/modeling-steps/2-dc-module-iv/point-value-models/sandia-pv-array-performance-model/.

[108] Boyson William Earl, Galbraith Gary M, King David L, Gonzalez Sigifredo. Performance model for grid-connected photovoltaic inverters. Sandia National Laboratories; 2007.

[109] Growitz A, Dierauf T, Kurtz S, Hansen C. Weather-Corrected Performance Ratio. NREL Technical Report NREL/TP-5200-57991 ", April 2013. [Online]. Available: http://www.nrel.gov/docs/fy13osti/57991.pdf.

[110] Sweerts Bart, Pfenninger Stefan, Su Yang, Folini Doris, van der Zwaan Bob, Wild Martin. Estimation of losses in solar energy production from air pollution in China since 1960 using surface radiation data. Nature Energy 2019/08/01 2019;4(8):657–63. https://doi.org/10.1038/s41560-019-0412-4.

[111] ninja Renewables. GSEE.", https://www.renewables.ninja/. [Accessed December 2021]. accessed.

[112] Wu Qiuxuan, et al. Quantifying Analysis of the Impact of Haze on Photovoltaic Power Generation. IEEE Access 2020;8:215977–86.

[113] Sheng Khoo Yong, et al. Optimal orientation and tilt angle for maximizing in-plane solar irradiation for PV applications in Singapore. IEEE Journal of photovoltaics 2013;4(2):647–53.

[114] Liu Benjamin YH, Jordan Richard C. The long-term average performance of flat-plate solar-energy collectors: with design data for the US, its outlying possessions and Canada. Solar energy 1963;7(2):53–74.

[115] Klucher TM. Evaluation of models to predict insolation on tilted surfaces. Solar Energy 1979/01/01/1979;23(2):111–4. https://doi.org/10.1016/0038-092X(79)90110-5.

[116] Temps Ralph C, Coulson KL. Solar radiation incident upon slopes of different orientations. Solar energy 1977;19(2):179–84.

[117] Fernández Eduardo F, Almonacid F, Mallick TK, Pérez-Higueras P. Analytical Modelling of High Concentrator Photovoltaic Modules Based on Atmospheric Parameters. International Journal of Photoenergy 2015:872163. https://doi.org/10.1155/2015/872163. 2015/02/23 2015.

[118] Fernández Eduardo F, Almonacid F, Rodrigo P, Pérez-Higueras P. Model for the prediction of the maximum power of a high concentrator photovoltaic module. Solar Energy 2013;97:12–8.

[119] NASA. Multi-Angle Implementation of Atmospheric Correction (MAIAC) (MCD19) (accessed April, 2022), https://modis-land.gsfc.nasa.gov/MAIAC.html.

[120] NASA. Ozone Monitoring Instrument (OMI) (accessed April, 2022), https://earthdata.nasa.gov/earth-observation-data/near-real-time/download-nrt-data/omi-nrt.

[121] NASA. GISS GCM ModelE. https://www.giss.nasa.gov/tools/modelE/. [Accessed April 2022].

[122] NASA. CERES Data Products. https://ceres.larc.nasa.gov/data/. [Accessed April 2022].

[123] NASA. Modern-Era Retrospective analysis for Research and Applications (MERRA). https://disc.gsfc.nasa.gov/datasets?project=MERRA. [Accessed April 2022].

[124] NASA. Modern-Era Retrospective analysis for Research and Applications, Version 2. https://disc.gsfc.nasa.gov/datasets?project=MERRA-2. [Accessed April 2022].

[125] Richard, Pfeifroth Müller Uwe, Träger-Chatterjee Christine, Cremer Roswitha, Trentmann Jörg, Hollmann Rainer. Surface Solar Radiation Data Set - Heliosat (SARAH) - Edition 1. https://doi.org/10.5676/EUM_SAF_CM/SARAH/V001.

[126] NASA. Nasa earth science data (accessed April, 2022), https://eospso.nasa.gov/content/nasa-earth-science-data.

[127] Dewan Nitika, et al. Stable isotopes of lead and strontium as tracers of sources of airborne particulate matter in Kyrgyzstan. Atmospheric Environment 2015/11/01/2015;120:438–46. https://doi.org/10.1016/j.atmosenv.2015.09.017.

[128] Bright Jamie M, Sun Xixi, Gueymard Christian A, Acord Brendan, Wang Peng, Engerer Nicholas A. Bright-Sun: A globally applicable 1-min irradiance clear-sky detection model. Renewable and Sustainable Energy Reviews 2020/04/01/2020;121:109706. https://doi.org/10.1016/j.rser.2020.109706.

[129] Gueymard Christian A. REST2: High-performance solar radiation model for cloudless-sky irradiance, illuminance, and photosynthetically active radiation–Validation with a benchmark dataset. Solar Energy 2008;82(3):272–85.

[130] Pierre Ineichen. A broadband simplified version of the Solis clear sky model. Solar Energy 2008;82(8):758–62.

[131] Rigollier Christelle, Bauer Olivier, Wald Lucien. On the clear sky model of the ESRA—European Solar Radiation Atlas—with respect to the Heliosat method. Solar energy 2000;68(1):33–48.

[132] Gueymard Christian A. Clear-sky irradiance predictions for solar resource mapping and large-scale applications: Improved validation methodology and detailed performance analysis of 18 broadband radiative models. Solar Energy 2012;86(8):2145–69.

[133] Pierre Ineichen, Perez Richard. A new airmass independent formulation for the Linke turbidity coefficient. Solar Energy 2002;73(3):151–7.

[134] Sun Xixi, Bright Jamie M, Gueymard Christian A. Xinyu Bai, Brendan Acord, and Peng Wang, "Worldwide performance assessment of 95 directand diffuse clear-sky irradiance models using principal component analysis. Renewable and Sustainable Energy Reviews 2021/01/01/2021;135:110087. https://doi.org/10.1016/j.rser.2020.110087.

[135] Zagouras Athanassios, Alexander Kolovos, Carlos F, Coimbra M. Objective framework for optimal distribution of solar irradiance monitoring networks. Renewable Energy 2015/08/01/2015;80:153–65. https://doi.org/10.1016/j.renene.2015.01.046.

[136] Nie Norman H, Bent Dale H, Hull C Hadlai. SPSS: Statistical package for the social sciences. New York: McGraw-Hill; 1975.

[137] Lars St, Wold Svante. Analysis of variance (ANOVA). Chemometrics and intelligent laboratory systems 1989;6(4):259–72.

[138] NREL. System Advisor Model (SAM) (accessed April, 2022), https://sam.nrel.gov/about-sam/sam-open-source.html.

[139] Shimokawa Ryuichi, Nagamine Fumiaki, Miyake Yukiharu, Fujisawa Kazuya, Hamakawa Yoshihiro. Japanese indoor calibration method for the reference solar cell and comparison with the outdoor calibration. Japanese journal of applied physics 1987;26(1R):86.

[140] Sandia National Laboratories. PV_LIB Toolbox for MATLAB. https://pvpmc.sandia.gov/applications/pv_lib-toolbox/. [Accessed December 2021]. accessed.

[141] pvlib. "pvlib python, https://pvlib-python.readthedocs.io/en/stable/. [Accessed December 2021].

[142] NASA CERES Science Team. CERES SYN1deg ", https://ceres.larc.nasa.gov/data/#syn1deg-level-3. [Accessed September 2021].

[143] Doelling David R, et al. Geostationary enhanced temporal interpolation for CERES flux products. Journal of Atmospheric and Oceanic Technology 2013;30(6):1072–90.
[144] ninja renewables. GSEE: Global Solar Energy Estimator. https://github.com/renewables-ninja/gsee.
[145] Pfenninger Stefan. GSEE: Global Solar Energy Estimator. https://github.com/renewables-ninja/gsee. [Accessed December 2021].
[146] King David L, Kratochvil Jay A, Earl Boyson William. Photovoltaic array performance model. United States. Department of Energy; 2004.
[147] Almonacid F, Pérez-Higueras PJ, Fernández Eduardo F, Rodrigo P. Relation between the cell temperature of a HCPV module and atmospheric parameters. Solar Energy Materials and Solar Cells 2012;105:322–7.
[148] Fernández Eduardo F, Almonacid F, Rodrigo P, Pérez-Higueras P. Calculation of the cell temperature of a high concentrator photovoltaic (HCPV) module: A study and comparison of different methods. Solar Energy Materials and Solar Cells 2014/02/01/2014;121:144–51. https://doi.org/10.1016/j.solmat.2013.11.009.
[149] Chatterjee Samprit, McLeish DL. Fitting linear regression models to censored data by least squares and maximum likelihood methods. Communications in Statistics-Theory and Methods 1986;15(11):3227–43.
[150] Ma Changfeng, Jiang Lihua. Some research on Levenberg–Marquardt method for the nonlinear equations. Applied mathematics and Computation 2007;184(2):1032–40.
[151] Son Junghoon, Jeong Sujong, Park Hayoung, Park Chang-Eui. The effect of particulate matter on solar photovoltaic power generation over the Republic of Korea. Environmental Research Letters 2020;15(8):084004.
[152] AirNow Department of State (DOS). Air quality data. accessed, https://airnow.gov/index.cfm?action=airnow.global_summary.
[153] China National Environmental Monitoring Centre (CNEMC). "China's Air Quality Data." accessed.
[154] London Air Quality and Network (LAQN). London's Air Quality data. accessed, http://www.londonair.org.uk/LondonAir/General/about.aspx.
[155] Red Automatica de and Monitoreo Atmosférico (RAMA). Mexico's Air Quality data. accessed, http://www.aire.df.gob.mx/default.phpopc=%27aKBh%27.
[156] California Air and Resource Board. California Air quality data. accessed, https://ww2.arb.ca.gov/.
[157] Nocerino M, et al. Assessing the Impact of Haze on Solar Energy Potential Using Long Term PM2. 5 Concentration and Solar Insolation Filed Data in Naples, Italy. Sensors and Microsystems 2020;125.
[158] Global Solar Atlas. Global Solar Atlas. accessed, globalsolaratlas.info.
[159] Zhang Yingchen, Yang Rui, Zhang Jie, Weng Yang, Bri-Mathias Hodge. Chapter 16 - Predictive Analytics for Comprehensive Energy Systems State Estimation. In: Arghandeh R, Zhou Y, editors. Big Data Application in Power Systems. Elsevier; 2018. p. 343–76.
[160] Hyndman Rob J, Khandakar Yeasmin. Automatic time series forecasting: the forecast package for R. Journal of statistical software 2008;27(1):1–22.
[161] Massaoudi Mohamed, Refaat Shady S, Chihi Ines, Mohamed Trabelsi, Oueslati Fakhreddine S, Abu-Rub Haitham. A novel stacked generalization ensemble-based hybrid LGBM-XGB-MLP model for Short-Term Load Forecasting. Energy 2021;214:118874.
[162] Yang Ying, Elia Campana Pietro, Yan Jinyue. Potential of unsubsidized distributed solar PV to replace coal-fired power plants, and profits classification in Chinese cities. Renewable and Sustainable Energy Reviews 2020;131:109967.
[163] Figueiredo Raquel, Nunes Pedro, Meireles Mónica, Madaleno Mara, Brito Miguel C. Replacing coal-fired power plants by photovoltaics in the Portuguese electricity system. Journal of Cleaner Production 2019;222:129–42.
[164] Holland Clift Dean, Suehrcke Harry. Control optimization of PV powered electric storage and heat pump water heaters. Solar Energy 2021;226:489–500.
[165] Mahmoudi Mohammad, Dehghan Maziar, Haghgou Hamidreza, Keyanpour-Rad Mansoor. Techno-economic performance of photovoltaic-powered air-conditioning heat pumps with variable-speed and fixed-speed compression systems. Sustainable Energy Technologies and Assessments 2021;45:101113.
[166] Pearce JM, Sommerfeldt N. Economics of Grid-Tied Solar Photovoltaic Systems Coupled to Heat Pumps: The Case of Northern Climates of the US and Canada. Energies 2021;14:834. Note: MDPI stays neutral with regard to jurisdictional claims in published … 2021.
[167] Padovani Filippo, Sommerfeldt Nelson, Longobardi Francesca, Pearce Joshua M. Decarbonizing rural residential buildings in cold climates: A techno-economic analysis of heating electrification. Energy and Buildings 2021;250:111284.
[168] Chukwu Uwakwe C, Mahajan Satish M. V2G parking lot with PV rooftop for capacity enhancement of a distribution system. IEEE Transactions on Sustainable Energy 2013;5(1):119–27.
[169] Kelly NJ, Allison J, Flett G, Hand JW. Assessing the ability of roof-mounted photovoltaic (PV) canopies to support electric vehicle (EV) charging in cities. uSIM2020 Building to Buildings–Urban and Community Energy Modelling; 2020.
[170] Sanjay Deshmukh Swaraj, Pearce Joshua M. Electric vehicle charging potential from retail parking lot solar photovoltaic awnings. Renewable Energy 2021;169:608–17.
[171] Shah Kunal K, George Dane, Swan Lukas, Pearce Joshua M. Performance and analysis of retail store-centered microgrids with solar photovoltaic parking lot, cogeneration, and battery-based hybrid systems. Engineering Reports 2021;3(11):e12418.
[172] Jäger-Waldau Arnulf. The untapped area potential for photovoltaic power in the European Union. Clean Technologies 2020;2(4):440–6.
[173] Li Guiqiang, Xuan Qingdong, Pei Gang, Su Yuehong, Lu Yashun, Ji Jie. Life-cycle assessment of a low-concentration PV module for building south wall integration in China. Applied energy 2018;215:174–85.
[174] Torres João Paulo N, et al. Effect of reflector geometry in the annual received radiation of low concentration photovoltaic systems. Energies 2018;11(7):1878.
[175] Hollman Madeleine R, Pearce Joshua M. Geographic potential of shotcrete photovoltaic racking: Direct and low-concentration cases. Solar Energy 2021;216:386–95.
[176] Andrews Rob, Pollard Andrew, Pearce Joshua. Photovoltaic System Performance Enhancement With Non-Tracking Planar Concentrators: Experimental Results and Bi-Directional Reflectance Function (BDRF) Based Modelling. In: IEEE 39th Photovoltaic Specialists Conference. PVSC); 2013.
[177] Andrews Rob W, Pollard Andrew, Pearce Joshua M. Photovoltaic system performance enhancement with non-tracking planar concentrators: Experimental results and BDRF based modelling. 2013. IEEE 39th Photovoltaic Specialists Conference (PVSC). IEEE; 2013. 0229-0234.
[178] Peters IM, Karthik S, Buonassisi T, Nobre A. The Impact of Fine Particular Matter (PM2.5) on Photovoltaic Energy Yield - A Study on the Example of New Delhi. IEEE 7th World Conference on Photovoltaic Energy Conversion (WCPEC) (A Joint Conference of 45th IEEE PVSC, 28th PVSEC & 34th EU PVSEC). 2018. p. 2581–3. https://doi.org/10.1109/PVSC.2018.8548110. 10-15 June 2018 2018.
[179] Wild Martin, et al. From dimming to brightening: Decadal changes in solar radiation at Earth's surface. Science 2005;308(5723):847–50.
[180] Wild Martin. Decadal changes in radiative fluxes at land and ocean surfaces and their relevance for global warming. Wiley Interdisciplinary Reviews: Climate Change 2016;7(1):91–107.
[181] Statista. Average number of people living in households in China from 1990 to 2020. https://www.statista.com/statistics/278697/average-size-of-households-in-china/. [Accessed April 2022].
[182] Statista. Total population of China from 1980 to 2021 with forecasts until 2026 (accessed April, 2022), https://www.statista.com/statistics/263765/total-population-of-china/.
[183] Statista. Household electricity consumption per capita in China from 2000 to 2018 ". https://www.statista.com/statistics/597852/household-consumption-of-electricity-per-capita-in-china/. [Accessed April 2022].
[184] Shaddick G, Thomas ML, Mudu P, Ruggeri G, Gumy S. Half the world's population are exposed to increasing air pollution. npj Climate and Atmospheric Science 2020/06/17 2020;3(1):23. https://doi.org/10.1038/s41612-020-0124-2.
[185] Allen Robert J, Landuyt William, Rumbold Steven T. An increase in aerosol burden and radiative effects in a warmer world. Nature Climate Change 2016/03/01 2016;6(3):269–74. https://doi.org/10.1038/nclimate2827.
[186] Pawluk Robert E, Chen Yuxiang, She Yuntong. Photovoltaic electricity generation loss due to snow–A literature review on influence factors, estimation, and mitigation. Renewable and Sustainable Energy Reviews 2019;107:171–82.
[187] Powers Loren, Newmiller Jeff, Townsend Tim. Measuring and modeling the effect of snow on photovoltaic system performance. 35th IEEE Photovoltaic Specialists Conference, 2010. IEEE; 2010. 000973-000978.
[188] Marion Bill, Schaefer Robert, Holden Caine, Sanchez Gonzalo. Measured and modeled photovoltaic system energy losses from snow for Colorado and Wisconsin locations. Solar Energy 2013;97:112–21.
[189] Andrews Rob W, Pollard Andrew, Pearce Joshua M. The effects of snowfall on solar photovoltaic performance. Solar Energy 2013;92:84–97.
[190] Heidari Negin, Gwamuri Jephias, Townsend Tim, Pearce Joshua M. Impact of snow and ground interference on photovoltaic electric system performance. IEEE Journal of Photovoltaics 2015;5(6):1680–5.
[191] Andrews Rob W, Pearce Joshua M. Prediction of energy effects on photovoltaic systems due to snowfall events. 38th IEEE Photovoltaic Specialists Conference, 2012. IEEE; 2012. 003386-003391.
[192] Government of India Ministry of New and Renewable Energy. Annula report 2016-17," 2016-17. [Online]. Available: https://mnre.gov.in/img/documents/uploads/file_f-1608050046985.pdf.
[193] Energy Portal China. Solar PV statistics. 2016. 2017 [Online]. Available: https://chinaenergyportal.org/en/2016-pv-installations-utility-distributed-province/.
[194] Zhang Chi, Li Wenyuan, Yu Juan, Xu Ruilin. Modeling impacts of PM 2.5 concentration on PV power outputs. International Conference on Probabilistic Methods Applied to Power Systems (PMAPS), 2016. IEEE; 2016. p. 1–7.
[195] Gupta Vinay, Sharma Madhu, Kumar Pachauri Rupendra, Dinesh Babu KN. Comprehensive review on effect of dust on solar photovoltaic system and mitigation techniques. Solar Energy 2019/10/01/2019;191:596–622. https://doi.org/10.1016/j.solener.2019.08.079.
[196] Khonkar Hussam, et al. Importance of cleaning concentrated photovoltaic arrays in a desert environment. Solar Energy 2014/12/01/2014;110:268–75. https://doi.org/10.1016/j.solener.2014.08.001.
[197] Alshawaf Mohammad, Poudineh Rahmatallah, Alhajeri Nawaf S. Solar PV in Kuwait: The effect of ambient temperature and sandstorms on output variability and uncertainty. Renewable and Sustainable Energy Reviews 2020;134:110346.
[198] Middleton Nick, Kang Utchang. Sand and Dust Storms: Impact Mitigation. Sustainability 2017;9(6):1053 [Online]. Available: https://www.mdpi.com/2071-1050/9/6/1053.
[199] Goudie Andrew S, Middleton Nicholas J. Dust storm control. Desert Dust in the Global System 2006:193–9.
[200] Muller Damon A. *Using Crime Prevention to Reduce Deliberate Bushfires in Australia* (no. 4). Australian Institute of Emergency Services; 2009. p. 27.
[201] Ducat Lauren, James R, Ogloff P. Understanding and Preventing Bushfire-Setting: A Psychological Perspective. Psychiatry, Psychology and Law 2011/08/01 2011;18(3):341–56. https://doi.org/10.1080/13218719.2011.598633.
[202] Ye BAI, WU Yingda, JIA Yisong, WANG Bo. Link Between Climate Anomaly and Australia Bushfires in 2019-2020. China Emergency Rescue. 2020. 02.

[203] Jan Van Oldenborgh Geert, et al. Attribution of the Australian bushfire risk to anthropogenic climate change. 2020.
[204] Global Communications Team. How these five global cities have improved their air quality." CityTalk. https://talkofthecities.iclei.org/how-these-five-global-cities-have-improved-their-air-quality/. [Accessed December 2021].
[205] Staff Reuters. China puts finishing touches to three-year smog crackdown plan." Reuters Staff (accessed Nov., 2021), https://www.reuters.com/article/us-china-pollution/china-puts-finishing-touches-to-three-year-smog-crackdown-plan-idUSKBN1FK095.
[206] phys.org. China says air quality 'improved' in. phys.org, https://phys.org/news/2018-01-china-air-quality.html. [Accessed November 2021].
[207] Kilinsky Jennifer. International climate change liability: A myth or a reality. J. Transnat'l L. & Pol'y 2008;18:377.
[208] Farber Daniel A. Tort law in the era of climate change, Katrina, and 9/11: Exploring liability for extraordinary risks. Val. UL Rev. 2008;43:1075.
[209] Heidari Negin, Pearce Joshua M. A review of greenhouse gas emission liabilities as the value of renewable energy for mitigating lawsuits for climate change related damages. Renewable and sustainable energy reviews 2016;55:899–908.
[210] Pascaris Alexis S, Pearce Joshua M. US greenhouse gas emission bottlenecks: Prioritization of targets for climate liability. Energies 2020;13(15):3932.
[211] Chen Yufeng, Zhu Zhitao. Liability Structure and Carbon Emissions Abatement: Evidence from Chinese Manufacturing Enterprises. Environmental and Resource Economics 2022:1–27.
[212] Harrington Luke J, EL Otto Friederike. Attributable damage liability in a non-linear climate. Climatic Change 2019;153(1):15–20.
[213] Farber Daniel A. The case for climate compensation: justice for climate change victims in a complex world, 377. Utah L. Rev.; 2008.
[214] Healy J Kevin, Tapick Jeffrey M. Climate change: it's not just a policy issue for corporate counsel-it's a legal problem. Colum. J. Envtl. L. 2004;29:89.
[215] Gupta Ridhima, Somanathan E, Dey Sagnik. Global warming and local air pollution have reduced wheat yields in India. Climatic Change 2017;140(3):593–604.
[216] Burney Jennifer, Ramanathan V. Recent climate and air pollution impacts on Indian agriculture. Proceedings of the National Academy of Sciences 2014;111(46):16319–24.
[217] Metaxoglou Konstantinos, Smith Aaron. Productivity spillovers from pollution reduction: reducing coal use increases crop yields. American Journal of Agricultural Economics 2020;102(1):259–80.
[218] Burney Jennifer A. The downstream air pollution impacts of the transition from coal to natural gas in the United States. Nature Sustainability 2020;3(2):152–60.
[219] Liu Xiang, Desai Ankur R. Significant reductions in crop yields from air pollution and heat stress in the United States. Earth's Future 2021;9(8):e2021EF002000.
[220] Zhang Tianyi, et al. Modeling the joint impacts of ozone and aerosols on crop yields in China: An air pollution policy scenario analysis. Atmospheric Environment 2021;247:118216.
[221] Prehoda Emily W, Pearce Joshua M. Potential lives saved by replacing coal with solar photovoltaic electricity production in the US. Renewable and Sustainable Energy Reviews 2017;80:710–5.
[222] Robbins Anthony. How to understand the results of the climate change summit: Conference of Parties21 (COP21) Paris 2015. Journal of Public Health Policy 2016/05/01 2016;37(2):129–32. https://doi.org/10.1057/jphp.2015.47.
[223] UNFCCC. Climate Change Conference (COP) 26 (accessed Nov., 2021), https://unfccc.int/conference/glasgow-climate-change-conference-october-november-2021.
[224] Watson Sterling, Bian David, Sahraei Nasim, Buonassisi Tonio, Marius Peters Ian. Advantages of operation flexibility and load sizing for PV-powered system design. Solar Energy 2018;162:132–9.
[225] Sahraei Nasim, Watson Sterling M, Anthony Pennes, Marius Peters Ian, Buonassisi Tonio. Design approach for solar cell and battery of a persistent solar powered GPS tracker. Japanese Journal of Applied Physics 2017;56(8S2). 08ME01.
[226] Cristaldi Loredana, et al. Economical evaluation of PV system losses due to the dust and pollution. IEEE International Instrumentation and Measurement Technology Conference Proceedings, 2012. IEEE; 2012. p. 614–8.
[227] Jones Russell K, et al. Optimized cleaning cost and schedule based on observed soiling conditions for photovoltaic plants in central Saudi Arabia. IEEE journal of photovoltaics 2016;6(3):730–8.
[228] Elias Urrejola, et al. Effect of soiling and sunlight exposure on the performance ratio of photovoltaic technologies in Santiago, Chile. Energy Conversion and Management 2016;114:338–47.
[229] Besson Pierre, Munoz Constanza, Ramirez-Sagner Gonzalo, Salgado Marcelo, Rodrigo Escobar, Werner Platzer. Long-term soiling analysis for three photovoltaic technologies in Santiago region. IEEE Journal of Photovoltaics 2017;7(6):1755–60.
[230] You Siming, Lim Yu Jie, Dai Yanjun, Wang Chi-Hwa. On the temporal modelling of solar photovoltaic soiling: Energy and economic impacts in seven cities. Applied Energy 2018;228:1136–46.
[231] Rodrigo Pedro M, Gutiérrez Sebastián, Micheli Leonardo, Fernández Eduardo F, Almonacid FM. Optimum cleaning schedule of photovoltaic systems based on levelised cost of energy and case study in central Mexico. Solar Energy 2020;209:11–20.
[232] Mazumder MK, Sharma R, Biris AS, Zhang J, Calle C, Zahn M. Self-cleaning transparent dust shields for protecting solar panels and other devices. Particulate Science and Technology 2007;25(1):5–20.
[233] Mazumder Malay, et al. Characterization of electrodynamic screen performance for dust removal from solar panels and solar hydrogen generators. IEEE Transactions on industry applications 2013;49(4):1793–800.
[234] Ju Fali, Fu Xiangzhao. Research on impact of dust on solar photovoltaic (PV) performance. International Conference on Electrical and Control Engineering. IEEE; 2011. p. 3601–6. 2011.
[235] Hamidon SNNA, Nawabjan A, Abdullah AS, Hussin SM, Ishak MHI. Reducing soiling issues on photovoltaic panels using hydrophobic self-cleaning coating. Journal of Sol-Gel Science and Technology 2021/06/01 2021;98(3):627–36. https://doi.org/10.1007/s10971-021-05525-x.
[236] Zhong Hong, Hu Yan, Wang Yuanhao, Yang Hongxing. TiO2/silane coupling agent composed of two layers structure: A super-hydrophilic self-cleaning coating applied in PV panels. Applied energy 2017;204:932–8.
[237] Brennan MP, AL Abramase, Andrews Rob W, Pearce Joshua M. Effects of spectral albedo on solar photovoltaic devices. Solar Energy Materials and Solar Cells 2014;124:111–6.
[238] Andrews Rob W, Pearce Joshua M. The effect of spectral albedo on amorphous silicon and crystalline silicon solar photovoltaic device performance. Solar Energy 2013;91:233–41.
[239] Russell Thomas CR, Saive Rebecca, Augusto Andre, Bowden Stuart G, Atwater Harry A. The influence of spectral albedo on bifacial solar cells: A theoretical and experimental study. IEEE Journal of photovoltaics 2017;7(6):1611–8.
[240] Riedel-Lyngskær Nicholas, et al. The effect of spectral albedo in bifacial photovoltaic performance. Solar Energy 2022;231:921–35.
[241] IRENA. Ranks countries/areas to their renewable energy power capacity or electricity generation (accessed Jan, 2022), https://www.irena.org/Statistics/View-Data-by-Topic/Capacity-and-Generation/Country-Rankings.
[242] Botero-Valencia JS, Mejia-Herrera M, Pearce Joshua M. Low cost climate station for smart agriculture applications with photovoltaic energy and wireless communication. HardwareX; 2022, e00296.